Chapter 5

DIRBE Data Products

5.1 Overview

Brief descriptions of the *DIRBE* data products were given in §1.3. To make the Annual Average Sky Maps and Solar Elongation (ε) = 90° Sky Maps network–accessible and easy to use, they were broken up into files containing data for individual wavelength bands. The Weekly Sky Maps, which are designed to preserve information about the temporal variation of sky brightness stemming from a variable viewing perspective relative to the interplanetary dust (IPD) cloud, and other relatively large files are available from the NSSDC on CD–ROMs or tape. The network–accessible data products may be obtained by anonymous ftp from `cobe.gsfc.nasa.gov`, or through the World Wide Web from the COBE Home Page (`http://www.gsfc.nasa.gov/astro/cobe/cobe_home.html`). Table 5.1-1 lists the data products, shows how they are divided into files, and indicates how the files may be obtained.

Final ("Pass 3B") versions of the Project Data Sets [1] described in §5.7 were released in March 1997. These **supersede the "Pass 2B" versions** and include calibration and data quality improvements. The most notable change compensates for an error made in our application of the Sirius spectrum to calibrate the Pass 2B products, Sirius being the source used for absolute calibration at the five shortest *DIRBE* wavelengths (see §4.5.3): Pass 3B 1.25 - 12 μm intensity values are 5% lower than the corresponding Pass 2B values. Further changes designed to improve the stability of the relative calibration as a function of time affected mainly the long wavelength photometry. Finally, a better algorithm was used to calculate weekly–averaged intensity values (see §4.7.9), yielding more reliable photometry. The resulting improvement can be seen in a small number of sparsely sampled pixels where the Pass 2B data were anomalous, especially at 60 and 100 μm.

In addition to the calibration and data processing refinements noted above, slight changes were made in the data file formats. Standard FITS readers will now properly interpret the "binned quantities" and $\Delta\,Time$ values in the Weekly Sky Maps, and the sky coordinates recorded in the Galactic Plane Maps, rendering sections 5.7.2.1, 5.7.2.2 and 5.7.4.1 obsolete. Also, the Beam Profile Maps are normalized and sampled differently.

[1] The version is specified in the FITS primary header.

Table 5.1-1: *DIRBE* data products

Product	Contents	# files	MB/file	Format	Distrib.[a] medium
Time–Ordered Data	Calibrated time–ordered data; 1 file per week of optimized cryogenic operation	41	190	Native	t
Calibrated Individual Observations (CIO)	$\frac{1}{8}$th sec sampled sky survey data listed in pixel order for each day of the cryogenic mission	285	60	FITS binary table	n,c,t
CIO Pixel Index	Specifies which pixels are covered in each daily CIO file, and which rows in the CIO file contain data for a given pixel	285	1	FITS binary table	n,c,t
Weekly Sky Maps	Weekly–averaged intensities for 10 bands and Stokes Q and U parameters for 1.25, 2.2, and 3.5 μm bands; 1 file per week	41	28	FITS binary table	n,c,t
DIRBE Calibrated Annual File (DCAF)	Merged, pixel–ordered, weekly–averaged intensities for cryogenic mission. One file per face of the skycube.	6	∼200	FITS binary table	n,c,t
DCAF Pixel Index	Specifies which rows in the DCAF file contain data for each *DIRBE* pixel, and for which weeks of the mission	6	1	FITS binary table	n,c,t
Annual Average Sky Maps	Average of intensities for all 10 bands over the entire cryogenic mission; 1 file per band	10	11	FITS binary table	n,c,t
$\varepsilon = 90°$ Sky Maps	Intensities for all 10 bands for the special case of $\varepsilon = 90°$; 1 file per band	10	13	FITS binary table	n,c,t
Galactic Plane Maps	Galactic Plane subset of the $\varepsilon = 90°$ Sky Maps; limited to a 6 month interval	1	6	FITS binary table	n,c,t
DIRBE Sky And Zodi Atlas (DSZA)	Augmented form of the DCAF; includes a modeled IPD intensity for each week and each wavelength.	6	∼200	FITS binary table	n,c,t
Pixel Index to DSZA	Analogous to the DCAF Pixel Index, but for the DSZA.	6	1	FITS binary table	n,c,t
Zodi–Subtracted Mission Average Maps (ZSMA)	Average sky brightness after removal of the *DIRBE* IPD model for each of the 10 wavelength bands	10	6.3	FITS binary table	n,c,t
Photometric Standard Values	Names, positions, and photometric data for the 92 objects used to establish the baseline relative celestial calibration system	1	0.01	FITS binary table	n,c,t
Solar System Objects Data	*DIRBE* observations of Mars, Jupiter, Saturn, Uranus, Ceres, Pallas, and Vesta, including flux density measurements and ancillary data	7	0.05	FITS binary table	n,c,t

Faint Source Model	Predicted contribution to the diffuse sky brightness due to (faint) stars and other discrete Galactic sources. Model sky maps at 1.25, 2.2, 3.5, 4.9, 12 and 25 μm .	6	5	FITS binary table	n,c,t
Beam Profiles	Effective two–dimensional shape of *DIRBE* beam for each detector	16	0.5	FITS image	n,c,t
Color Corrections	Color correction factors needed in case source spectrum is not νI_ν = constant	1	0.04	ASCII	n,c,t
System Responses	Normalized system spectral response functions for each wavelength band	1	0.06	ASCII	n,c,t

[a] Data available from the NSSDC on tape (t), CD–ROM (c), or by anonymous ftp over the network (n).

5.2 Creation of *DIRBE* Data Products

Telemetry data from the *DIRBE* instrument were calibrated and converted to useful data products via the sequentially executed set of programs described in Chapter 4. This section briefly describes the processing steps that led to the creation of the individual data products.

5.2.1 Initial Pipeline Processing Stages

The unprocessed *DIRBE* science data consisted of consecutive $\frac{1}{8}$–second sampled observations of the sky brightness. At the survey scan rate, point sources were visible in the field of view for 0.3 s, during which time 2.4 samples were obtained. The attitude solution used to determine the line–of–sight for each sample was based upon data from the spacecraft Sun and Earth sensors and gyros, with fine corrections based upon the locations of isolated bright stars detected in the *DIRBE* 2.2 μm band. The rms accuracy of the attitude solution is approximately $1.5'$. Sky observations were routinely interrupted when the *COBE* spacecraft passed through the South Atlantic Anomaly (SAA) or when the instrument calibration stability was checked. The time–ordered sky observations had instrument offset signals removed and were calibrated photometrically relative to the *DIRBE* Internal Reference Source (IRS) (see §4.5). They were then made into daily sky maps by associating each sample with a pixel on the sky. Pixel area and location were determined according to the adopted map projection, the *COBE* Quadrilaterilized Spherical Cube (CSC) in ecliptic J2000 coordinates (see §5.3). On average, in that half of the sky covered, each pixel in a daily sky map was observed about 2.4 times, but the sampling was much denser for pixels near the edges of the viewing swath (solar elongation angles near 64° and 124°) than for those near the middle (see §3.1.2).

5.2.2 Creation of Calibrated Individual Observations

The photometric data in the daily sky maps described in §5.2.1 were corrected for the subsequently determined long–term response trends and absolute calibration factors in order to create the Calibrated Individual Observations (CIO) files. Observations made while the *COBE* was in the SAA, or when the data from *all* detectors are of low quality, were omitted. The photometric and ancillary data are organized in wavelength band order rather than in the original MUX sequence, and are presented in FITS binary tables (see §5.4). A pixel index file was prepared for each CIO file to facilitate retrieval of desired data.

5.2.3 Creation of Weekly Sky Maps

The *DIRBE* daily sky maps were averaged to make Weekly Sky Maps as follows. First, long–term gain stabilization corrections based upon repeated observations of stable celestial sources were applied, and the data were converted from instrumental units to calibrated specific intensities in MJy/sr (see §4.5.3.3). Data collected when the *COBE* spacecraft was in the SAA or when the *DIRBE* line–of–sight was close to the Moon, Mars, Jupiter, Saturn, Neptune, Uranus, or a bright comet or asteroid were excluded (see §4.7). Consequently, there are small holes in the *DIRBE* Weekly Sky Maps corresponding to these times. The remaining observations were then averaged to derive the quoted intensity at each pixel and wavelength; a robust averaging technique was employed (§4.7.9) to reduce the effects of outliers. The polarization channel intensities were converted to Stokes Parameters, Q and U, using the algorithm described in §4.6. If for some reason it was not possible to derive a reliable average intensity or Stokes parameter value for a given pixel, then a standard value less than -16375 was substituted for the real data. The mean time of observation and the mean solar elongation angle for each pixel were also recorded in the Weekly Sky Maps.

5.2.4 Creation of DIRBE Calibrated Annual File

One of the last steps in the *DIRBE* processing pipeline is to merge all weekly–averaged photometry into a single master file, and sort the data in ascending pixel–number order. This file, referred to as the *DIRBE* Calibrated Annual File, or DCAF, gives a pixel–by–pixel view of the intensity variations seen as a function of time. To create a DCAF data product, the master file was divided into six segments, one for each face of the *COBE* Sky Cube (see §5.3), and presented in FITS binary table format (see §5.4).

Each DCAF FITS file is accompanied by a pixel index file, which can be used to access the data corresponding to specific pixels without scrolling through the entire DCAF file.

5.2.5 Creation of Annual Average Sky Maps

At each wavelength, an Annual Average Sky Map was made by averaging the 41 Weekly Sky Maps that covered the cryogenic mission. In calculating the average, each Weekly Sky Map pixel (at each wavelength) was assigned a weight based on the number of times the pixel was observed. Information about the depth of sky coverage over the whole cryogenic mission is included in the Annual Average Sky Maps.

5.2.6 Creation of $\varepsilon = 90^\circ$ Sky Maps

At the ecliptic equator, solar elongations angles, ε, ranging from 64° to 124° were observed. In principle (except for gaps in coverage due to SAA passages, instrument calibration, etc.), every celestial line of sight was viewed by the *DIRBE* through the IPD cloud at 90° solar elongation once every 6 months, and hence once or twice during the 10–month cryogenic mission. When two $\varepsilon = 90^\circ$ observations were made, different foreground brightness values were observed at the two epochs since generally the Earth was not at the same heliocentric distance at these times, and also because the IPD cloud is not perfectly symmetric around the Sun or the ecliptic plane. The $\varepsilon = 90^\circ$ Sky Maps provide the 10 intensity values for each $\varepsilon = 90^\circ$ epoch observed for each pixel.

To be precise, few pixels were observed when the solar elongation angle was *exactly* 90°. To create the $\varepsilon = 90^\circ$ Sky Maps, the weekly–averaged intensities were monitored as a function of ε as time progressed and then interpolated to $\varepsilon = 90^\circ$. Specifically, a straight line was fitted to $I_\nu(\varepsilon; \lambda, \beta)$ vs. $[\frac{90}{\varepsilon} - 1]$ and the y–intercept was adopted as the $\varepsilon = 90^\circ$ intensity at nominal frequency ν and ecliptic coordinates (λ, β). Figure 5.2-1 shows the variation of brightness with ε for a representative pixel. The quantity $[\frac{90}{\varepsilon} - 1]$ was used instead of ε as the independent variable because the brightness was found to vary more linearly with the former than with the latter. Only observations made within ± 19 days of the $\varepsilon = 90^\circ$ point at each pixel were fitted, a restriction that also ensured a more linear trend; the effect was to exclude data obtained when the line of sight came close to the Sun ($\varepsilon \sim 64^\circ$), where $\frac{\partial^2 I_\nu}{\partial \varepsilon^2}$ was relatively large. The weight assigned to each weekly–averaged intensity was based on the standard deviation of the weekly–averaged value, σ_{I_ν}. When the weekly–averaged intensity value resulted from 5 or fewer observations, then the weight for that observation was based on $0.01 I_\nu$ or σ_{I_ν}, whichever was greater.

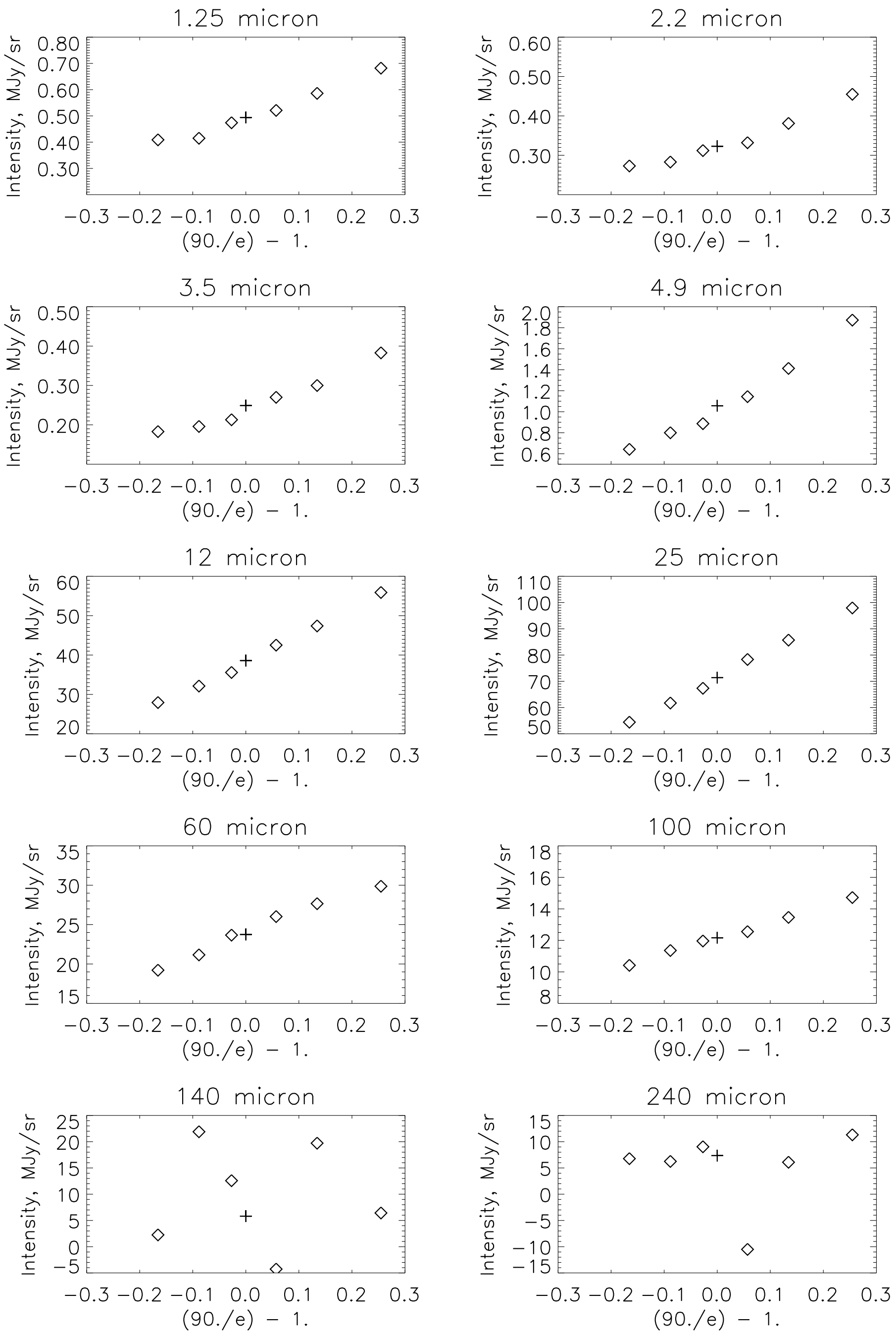

Figure 5.2-1: I_ν *vs.* $(90/\varepsilon - 1)$ for *DIRBE* pixel number 247071 at $(\lambda, \beta) \simeq (198^\circ\!.3, 1^\circ\!.1)$. The $\diamond$ symbols designate weekly–averaged *DIRBE* observations and the + symbols represent the interpolated intensities.

The standard deviation assigned to the interpolated intensity was the formal statistical error in the intercept at $\varepsilon = 90°$. The model error used to calculate the quoted χ^2 did not take into account sources of systematic error such as uncorrected nonlinearity or confusion noise. Hence, the quoted χ^2 values do not always accurately reflect the goodness of fit.

When the interpolated value was negative, which sometimes occurred in regions of low brightness (particularly at 140 and 240 μm, where the signal–to–noise ratio was low in a single week), the weighted average intensity was quoted instead of the interpolated value.

In some cases, weekly–averaged data were not available (either because of data processing constraints or the observational strategy), and the $\varepsilon = 90°$ intensity was obtained by extrapolating outside the range of elongation angles observed. Such cases include:

- pixels that would have been observed at $\varepsilon = 90°$ during the very beginning or very end of the cryogenic mission;
- a small number of pixels near the ecliptic plane where observations made at a solar elongation angle close to 90° were discarded due to close proximity of the Moon or Jupiter to the line of sight;
- pixels for which several weeks of observations were discarded because they consistently fell within SAA passages or instrument calibration periods; and
- pixels that would have been observed at $\varepsilon = 90°$ during the days (yyddd) 90110 – 90135 and 90217 – 90242 but were undersampled due to a suspension of normal observations while JFET–off tests were conducted (see §3.3.2.2).

Extrapolated values were included in the $\varepsilon = 90°$ Sky Maps only if two conditions were met:

1. intensity measurements were available for elongation angles within 5° of $\varepsilon = 90°$; and
2. the extrapolation interval in ε did not exceed one–third of the interval over which intensity measurements were available.

For the special case of an extrapolation within 1° of either ecliptic pole, the weighted average intensity was quoted.

Pixels with extrapolated intensities are flagged in the Photometric Quality field (FITQUAL for the $\varepsilon = 90°$ Sky Maps; the first byte of PHOTQUAL for the Galactic Plane Maps; see §5.7). Note that, because extrapolation was permitted, some of the times recorded in the $\varepsilon = 90°$ Sky Maps lie outside the temporal boundaries of the actual *DIRBE* mission.

In a limited number of cases, neither an interpolated nor a reliable extrapolated value could be computed. These cases include:

- pixels that would have been observed at $\varepsilon = 90°$ during the very beginning or very end of the cryogenic mission; and
- pixels for which photometry was unavailable or flagged as "bad" in a particular band for three or four successive weeks. This condition had the greatest impact at 100 μm (see §3.5.1).

In these cases, the $\varepsilon = 90°$ Sky Map value was set to a number less than or equal to -16375.

5.2.7 Creation of the Galactic Plane Maps

The Galactic Plane Maps are subsets of the $\varepsilon = 90°$ Sky Maps constrained spatially and temporally as follows:

- only pixels whose Galactic coordinates satisfy the conditions $-10° < b < +10°$ for $30° < \ell < 330°$, and $-15° < b < +15°$ at Galactic longitudes within 30° of the Galactic center are included; and

- only $\varepsilon = 90°$ intensity values applicable to the 6–month interval between 1990 January 1 and 1990 July 2 inclusive are provided; thus, a single intensity value is recorded per pixel (unlike the $\varepsilon = 90°$ Sky Maps; see §5.2.4). The time range was chosen to assure that map discontinuities in the foreground brightness due to differences in the Earth's orbital position at the time of observation would occur only along two boundaries (see §5.6.1).

5.2.8 Creation of *DIRBE* Sky and Zodi Atlas (DSZA)

An abridged version of the *DIRBE* Calibrated Annual File (DCAF) data set was merged with model zodiacal brightness values to create the *DIRBE* Sky and Zodi Atlas (DSZA). The zodiacal light intensity was computed using the *DIRBE* Interplanetary Dust (IPD) model (Kelsall *et al.* 1998). Data and model intensities from all 10 full–intensity wavelength bands appear in the DSZA.

To create the DSZA, selected fields were copied from each row of the DCAF table, and, if the quality of the copied photometry met certain specifications, then the corresponding zodiacal light contribution was computed and attached. Data obtained during certain time intervals with particular detectors were deemed to be of low quality. This includes weekly averaged photometry from Bands 1 through 8 for weeks 24 (90120–90126), 39 (90225–90231) and 40 (90232–90238), owing to the instrument testing that was done during these periods (see §3.3.2). The Band 8 photometry was also poor during week 4 (89345-89351), as the procedure for annealing the 100μm detector following SAA passages had not yet been finalized. In these cases, the photometry was recorded in the DSZA, but the zodiacal light contribution was not computed, as is indicated by the sentinel value -16999 in the table. For all other weeks and wavelengths, and in all pixels, a model zodiacal light intensity was recorded in the DSZA, even if the photometry was considered deficient.

To calculate the zodiacal light intensity, the DIRBE IPD Model was evaluated at a spatial position corresponding to the pixel number at the time that position was observed (`Time + Delta-Time`), and at each wavelength. The DIRBE IPD Model, a semi–physical parameterized model, is described in detail by Kelsall *et al.* (1998). Thermal and scattering source terms were integrated along each line of sight to compute the model intensities. The computed model brightness is color corrected (see §5.5 and Chapter 4) (*i.e.,* evaluated as if observed with the appropriate *DIRBE* bandpass, assuming an energy distribution $\nu I_\nu = constant$), putting it on an equal footing with the observations. Thus the model intensities and photometry values listed in the DSZA can be compared directly.

5.2.9 Creation of Zodi–Subtracted Mission Average (ZSMA) Maps

The ZSMA Maps are derived from the *DIRBE* Sky and Zodi Atlas (DSZA). For each pixel and wavelength, the tabulated zodical light (ZL) contribution is subtracted from each valid weekly photometric measure. To a good approximation, this has the effect of removing apparent time variations from the observed sky brightness. The individual weekly ZL–subtracted intensity values are then averaged over the entire cryogenic mission, yielding ten zodiacal light subtracted maps, one for each of the *DIRBE* full–intensity wavelength bands.

All of the weekly ZL–subtracted intensity values included in the average were assigned equal weights, however certain high–quality observations were excluded from the ZSMA to mitigate the effects of known imperfections in the IPD Model at extreme solar elongation angles. At $|\beta| \lesssim 60°$ the observations for which $\varepsilon < 68°$ or $\varepsilon > 120°$ were excluded. At higher ecliptic latitudes, in order to avoid discontinuities at $|\beta| \sim 60°$, the clipping at extreme solar elongation angles was gradually tapered to "zero clipping" at the poles.

5.3 Pixelization and the Quadrilateralized Spherical Cube Projection

A quadrilateralized spherical projection and a quad–tree pixelization scheme were adopted for all *COBE* sky maps, including the *DIRBE* maps. The so–called "*COBE* Quadrilateralized Spherical Cube" (CSC) is an approximately equal–area projection (to within a few percent) in which the celestial sphere is projected onto an inscribed cube. An advantage of the CSC over the Aitoff, Mollweide and Global–Sinusoidal projections is that polar singularities are avoided. A disadvantage is that there is no standard way to present data in the quad–cube projection in a FITS file. To maintain the best possible photometric integrity, the data products should be kept in their native projection for analysis. If reprojection is desired, it is recommended that quantities such as color temperatures be derived first.

Figure 5.3-1 depicts the CSC projection. The coordinate system is Geocentric Ecliptic J2000. The ecliptic plane runs horizontally through the middle of the unfolded cube. The North Ecliptic Pole is centered on "face 0" and the South Ecliptic Pole is centered on "face 5." The *DIRBE* convention is to divide each cube face into 256 × 256 pixels; thus, all–sky maps have $256^2 \times 6 = 393216$ pixels. Each pixel is approximately 0.32° on a side. Figure 5.3-2 illustrates the pixel numbering scheme.

CSC pixel numbers are used in the *DIRBE* Sky Map FITS files to convey spatial pointing information. Except for the Galactic Plane Maps, which provide sky coordinates as well as pixel numbers, the pixel number is the *only* pointing information provided in the map products. FORTRAN and IDL programs that convert pixel numbers to ecliptic, Galactic, or equatorial coordinates are described in Appendix D (see §§D.1.2 and D.1.3) and available on line through the *COBE* Home Page (`http://www.gsfc.nasa.gov/astro/cobe/cobe_home.html`). A related ancillary information file called `DIRBE_SKYMAP_INFO.FITS` is described in §5.3.1.

The Weekly Sky Maps and Annual Average Sky Maps give more precise pointing information in the form of a "pixel subposition" (see Tables 5.7-7 and 5.7-14). The subposition specifies a location within a 16 × 16 element grid superposed on a pixel. Numbers ranging from 0 to 255 are assigned to the grid positions according to the standard quad–tree rules described below.

5.3.1 Description of the File DIRBE_SKYMAP_INFO.FITS

An ancillary information file called `DIRBE_SKYMAP_INFO.FITS` explains the quad–tree scheme that relates CSC pixel numbers to (x,y) positions within the quad–sphere cube faces and tabulates the ecliptic J2000, Galactic (ℓ_{II}, b_{II}) and equatorial J2000 coordinates corresponding to the *DIRBE* pixel centers. This file may be obtained from the directory `cobe/general_information/skymap_info` at the anonymous ftp site `nssdca.gsfc.nasa.gov`.

The file has two parts: (1) a primary data array which is stored as a standard FITS image, and (2) a binary table extension. The 3–dimensional primary data array gives a rasterized 256 × 256 pixel image of each of the six CSC cube faces showing the *DIRBE* pixel numbers. The binary table lists the sky coordinates corresponding to the center of each *DIRBE* pixel and can substitute for the software described above.

Key elements of the quad–sphere projection and quad–tree pixelization scheme are explained in `COMMENT` lines in the main and extension FITS headers. For convenience, the remainder of this section contains excerpts from the header documentation.

Quadrilateralized spherical cube faces are tangent plane projections of the celestial sphere. In the quad–sphere projection, pixels are equally spaced and have approximately equal area on the cube and on the sky. The COBE quadrilateralized spherical cube (CSC) projection conserves area to approximately 1% across the whole cube with a maximum discrepancy from equal area of only a few percent at the edges of the cube. Furthermore, the projection distorts shapes minimally. Beam shapes or point response functions will differ only slightly depending upon location on the quad–cube face.

In the quad–tree nearest neighbor pixel numbering scheme, which is hierarchical, the pixel numbers are not sequential along a row or column. As presented in the primary data array, the first row of pixel numbers on a face is at the bottom, the last row is at the top, and the first pixel per face is in the lower right corner. The cube faces are numbered 0 through 5 corresponding to planes 1 through 6 (`NAXIS3`) in the primary data array, respectively. The *COBE* FITS keyword `PIXINDEX` is a CSC resolution index. It is defined such that $2^{(PIXINDEX-1)}$ specifies the dimension of a side of each square face, 256 pixels in the case of *DIRBE*. The dimension implied by `PIXINDEX` is recorded in the primary header keywords `NAXIS1` and `NAXIS2`.

An all–sky, skyward–looking, unfolded cube can be constructed by arranging the cube faces as follows (also see Figure 5.3-1):

0

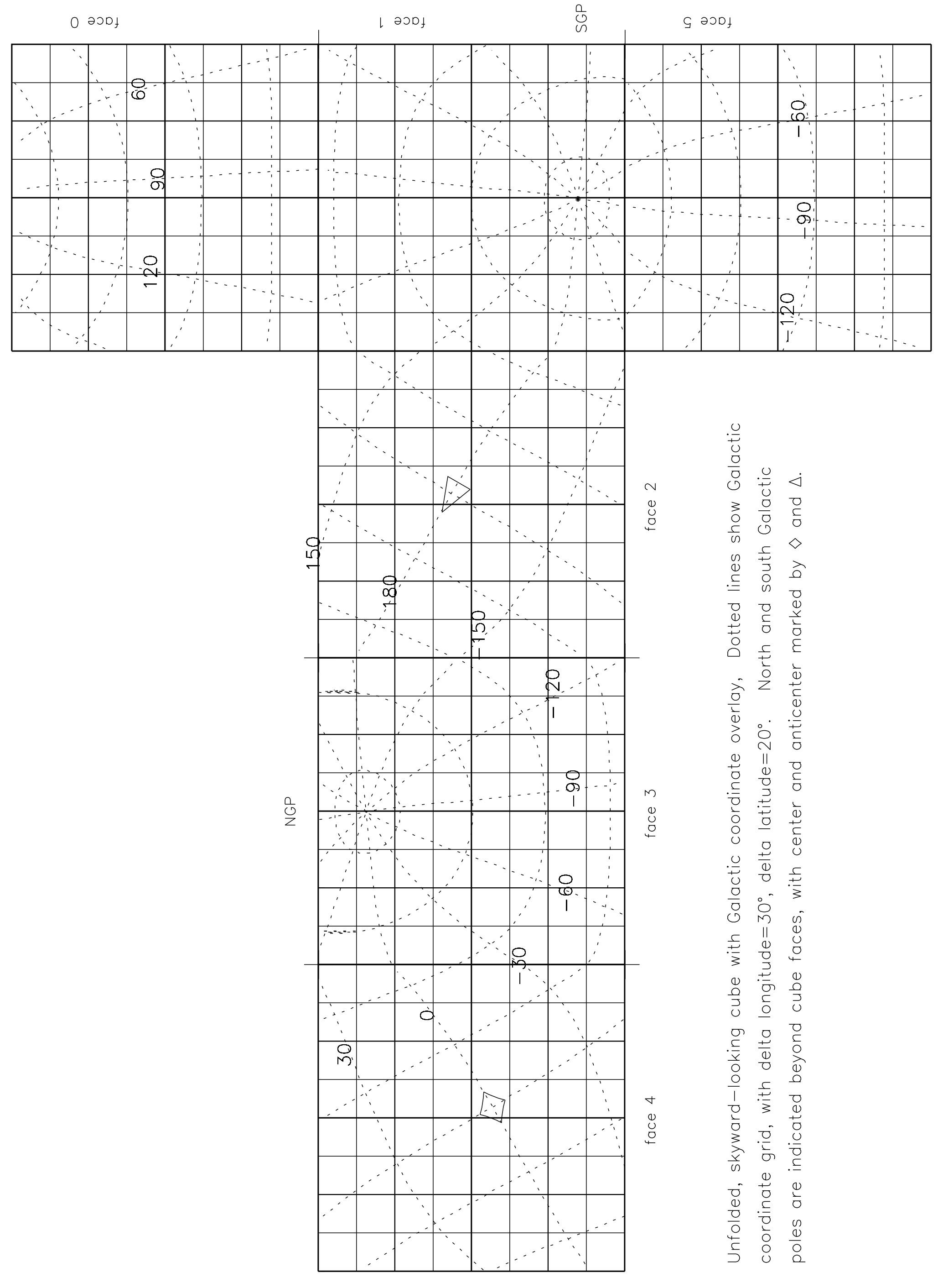

Figure 5.3-1: Unfolded, skyward–looking cube in ecliptic coordinates with Galactic coordinate overlay.

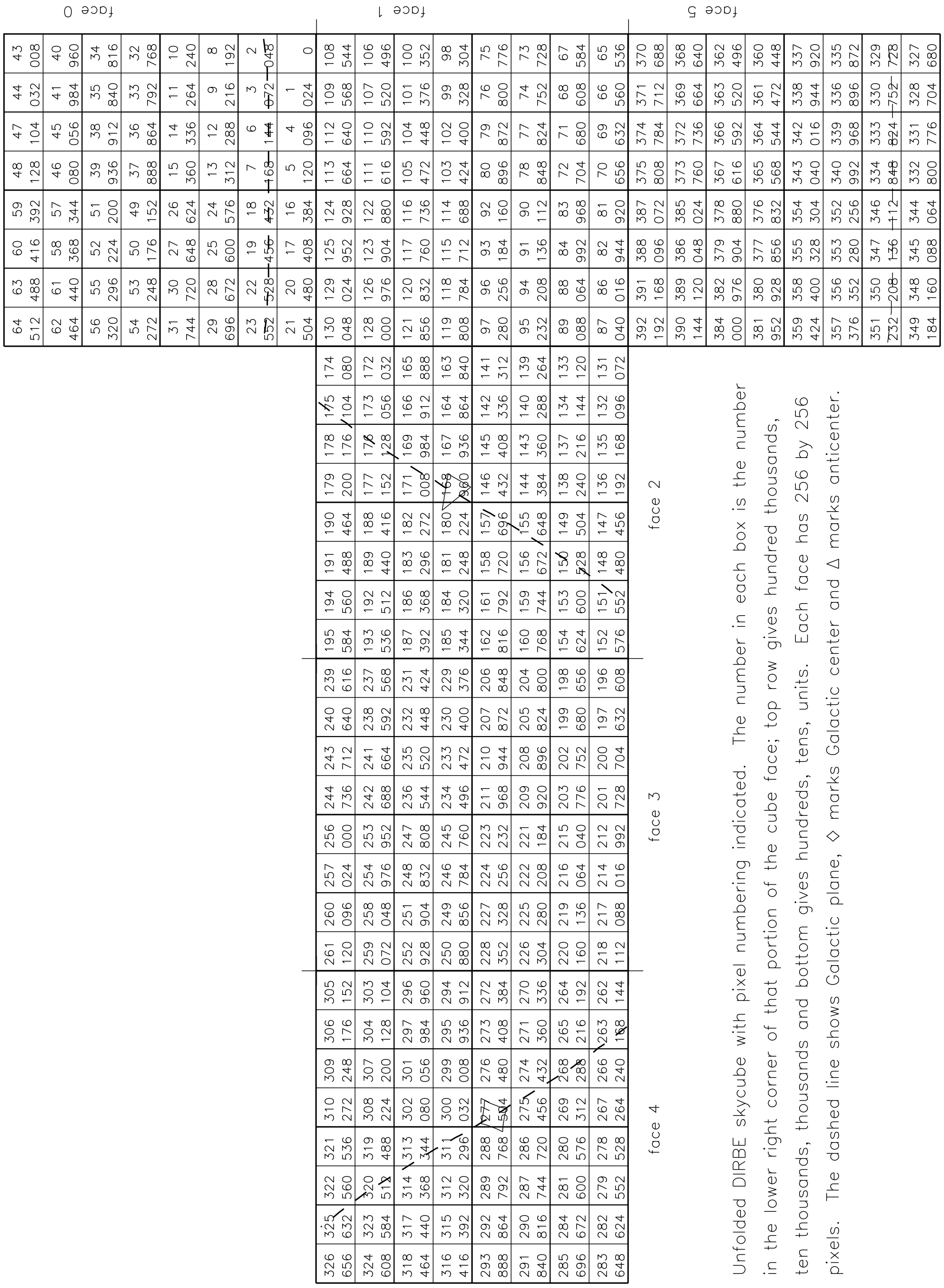

Figure 5.3-2: The *DIRBE* pixel numbering scheme in the quadrilateralized spherical cube projection.

```
4   3   2   1
            5
```

In the following equivalent arrangement, `b` denotes blank areas and `NAXIS1` = `NAXIS2` = 256:

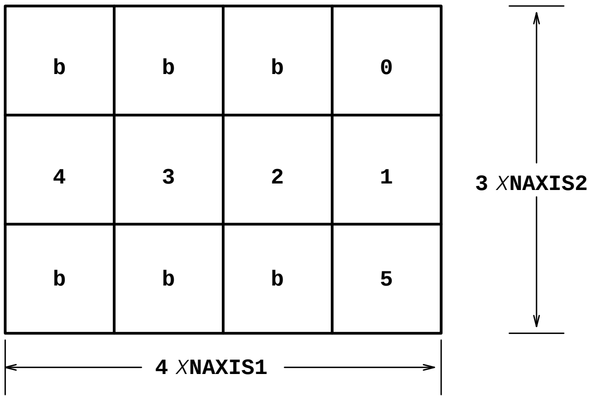

COBE data can be displayed on this unfolded cube by arranging the pixels in a binary table as they are arranged in the primary array of this file. For example, consider a sky map that contains the following data in a FITS binary table:

Pixel number	Signal	Error	Ecliptic longitude	Ecliptic latitude
0	22	1	315°.0	36°.7
1	43	2	317.9	38.1
2	36	2	312.1	38.1
3	31	1	315.0	39.7
⋮	⋮	⋮	⋮	⋮

Then the signal values will be mapped into the sites of the corresponding pixel numbers given in face 0 (*i.e.,* the first plane) of the primary array with the following result:

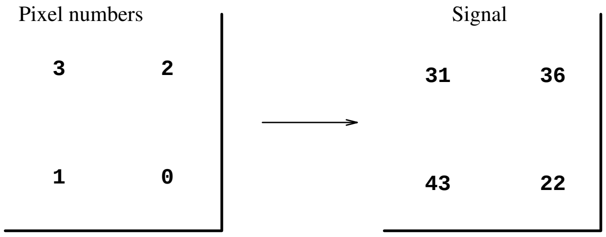

This illustrates the quad–tree pixelization scheme in which pixel numbers begin in the lower right corner of a cube face and increase from right to left and bottom to top. This "Z" pattern is repeated throughout a face as shown below for the lower right corner of face 0:

								y
63	62	59	58	47	46	43	42	7
61	60	57	56	45	44	41	40	6
55	54	51	50	39	38	35	34	5
53	52	49	48	37	36	33	32	4
31	30	27	26	15	14	11	10	3
29	28	25	24	13	12	9	8	2
23	22	19	18	7	6	3	2	1
21	20	17	16	5	4	1	0	0
x 7	6	5	4	3	2	1	0	

Z pattern

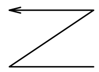

The quad-tree pixel ordering scheme is related to rasterized rectangular array positions as follows. The location within a face is specified by the $2^{(PIXINDEX-1)}$ least significant bits. The most significant bits identify the cube face as described below. The even least significant bits $(0, 2, \ldots, 2(PIXINDEX - 2))$ specify the x, or horizontal, raster position, and the odd bits $(1, 3, \ldots, (2\,PIXINDEX) - 3)$ specify the y position. Changing the pixel resolution thus simply requires adding or deleting pairs of least significant bits; each pair represents a resolution change in the x and y face coordinates by a factor of 2.

For example, for a `PIXINDEX` value of 4, the quad–tree pixel 24 (in binary) is

```
0 1 1 0 0 0
y x y x y x
```

Extracting the even and odd least significant bits gives

```
y = 010 = 2
x = 100 = 4
```

Thus, writing the pixel numbers in binary form clarifies the mapping hierarchy:

									Row
	111111	111110	111011	111010	101111	101110	101011	101010	7
	111101	111100	111001	111000	101101	101100	101001	101000	6
	110111	110110	110011	110010	100111	100110	100011	100010	5
	110101	110100	110001	110000	100101	100100	100001	100000	4
	011111	011110	011011	011010	001111	001110	001011	001010	3
	011101	011100	011001	011000	001101	001100	001001	001000	2
	010111	010110	010011	010010	000111	000110	000011	000010	1
	010101	010100	010001	010000	000101	000100	000001	000000	0
Bit #	543210	543210	543210	543210	543210	543210	543210	543210	
Column	7	6	5	4	3	2	1	0	

The separating lines above show how the hierarchy is built up.

As illustrated below, a cube face is bisected $(PIXINDEX - 1)$ times to reach the pixel resolution. In the following picture, a face at a PIXINDEX of 4 is depicted:

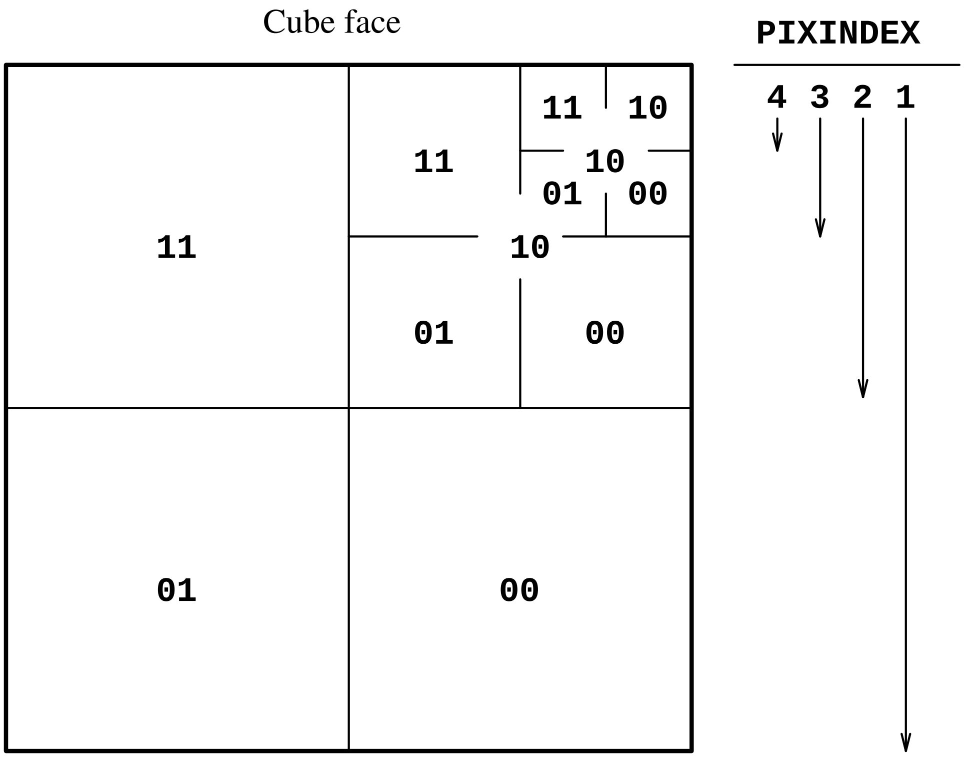

The face index is specified in the Most Significant Bits, that is, in bits $2(PIXINDEX - 1)$ through $2\,PIXINDEX$. Thus for pixel 24 on face 0 the binary number would be

```
 0 0 0    0 1 1 0 0 0     ,
| Face | Pixel number |
```

whereas for pixel number 24 on face 5 the binary number would be

```
 1 0 1    0 1 1 0 0 0     .
| Face | Pixel number |
```

The pixel numbers run sequentially from 0 on face 0 to $(NAXIS1 \times NAXIS2 \times NAXIS3) - 1$ on face 5. The last pixel number in a face is (facenumber + 1) $\times 2^{[2(PIXINDEX-1)]} - 1$. The first pixel number in a face is 0 for face 0, and 1 plus the last pixel number in the previous face for the other faces. Thus, for a PIXINDEX value of 4, pixel 24 on face 5, would be number 344 (binary 101011000 = decimal 344) with respect to the whole cube.

World coordinates such as ecliptic, equatorial, and Galactic are *not* linear across the *COBE* sky cube. The CSC is defined using the ecliptic J2000 reference frame. Cube face 0 is centered on the North ecliptic pole (NEP), faces 1 through 4 lie along the ecliptic plane (each spanning 90 degrees of ecliptic longitude), and face 5 is centered on the South ecliptic pole (SEP). Ecliptic longitude increases from face 1 to face 4. The vernal equinox lies at the center of face 1. Face 1 spans ecliptic longitudes from $-45°$ (*i.e.,* $315°$) to $+45°$. The anti–vernal equinox point is at the center of face 3. Faces 1–4 include the ecliptic latitudes ranging from roughly $-45°$ to $+45°$. Face 0 covers all ecliptic longitudes and latitudes around the North ecliptic pole down to approximately $+45°$. Face 5 covers all ecliptic longitudes and latitudes around the South ecliptic pole up to approximately $-45°$. The latitude ranges in each face are not exact because of the curvilinear nature of the coordinates on the CSC.

As shown in Figure 5.3-1, the North Galactic pole is on face 3 at J2000 ecliptic longitude 179.°32095 and latitude 29.°811954, and the Galactic center is on face 4 at J2000 ecliptic longitude 266.°14097 and latitude $-5\overset{\circ}{.}52967943$. The South Galactic pole is on face 1, and the Galactic anti–center is on face 2. Pixel numbers for these locations can be found in the `DIRBE_SKYMAP_INFO.FITS` binary table.

The North celestial pole is at ecliptic coordinates $(90\overset{\circ}{.}0, 66\overset{\circ}{.}5607089)$ and is located on face 0.

5.4 Data Product Formats

With a few exceptions, noted below, the data products are given in FITS format to enable their use in a variety of computing environments. The FITS standards and conventions are specified in *Definition of the Flexible Image Transport System (FITS)* and *A User's Guide for the Flexible Image Transport System (FITS),* both of which are available at `http://www.gsfc.nasa.gov/astro/fits/fits_home.html`. Appendix D.1 provides advice on how to read FITS data.

5.4.1 FITS Binary Table Extension

All of the *DIRBE* Sky Maps, the CIO, the DSZA and DCAF files, the Faint Source Model, the Solar System Objects Data, and the Photometric Standard Values are in FITS Binary Table extension format; they are not two–dimensional images. This format is reasonably compact and recognized by software that is readily available and in widespread use. In most cases, the rows of the FITS table correspond to pixels (*i.e.,* locations in the sky) and are organized in ascending pixel number order. Standard FITS–reading software provides the capability to select data from either a column of a FITS table (*e.g.,* intensity at a particular wavelength) or a row (*e.g.,* energy distribution at a particular direction). Thus, for example, it is straightforward to extract the 10–band spectral energy distribution in a particular pixel from the *DIRBE* Galactic Plane Maps file.

5.4.2 FITS Image Format

The Beam Profile Maps are stored as FITS images. A FITS–reading subroutine will return a two–dimensional array, and the FITS header provides coordinate information for the axes.

5.4.3 Native Binary Format

The Time–Ordered Data files are available in their original format: binary files of fixed record length. Since the data were processed on a VAX computer, floating point numbers do not conform to IEEE convention. The TOD file format is described in detail in a file called `DIRBE_TOD_RECORD_STRUCTURE.ASC`.

5.4.4 ASCII

System Spectral Response Functions, Color Correction Tables, and the *DIRBE* Beam Parameters table (Table 4.2-1) are provided in flat ASCII files to facilitate their incorporation into user programs.

5.5 Color Corrections

Following the *IRAS* convention (see the *"IRAS Catalogs and Atlases Explanatory Supplement,"* p. VI–27), the *DIRBE* spectral intensity data, I_ν, are expressed in MJy/sr at fixed nominal frequencies, assuming the source spectrum is νI_ν = constant (*i.e.*, constant intensity per logarithmic frequency interval). Where this is not true, a color correction must be applied to obtain an accurate intensity. The color correction factor, K, is defined such that

$$I_{\nu_0}(\text{actual}) = I_{\nu_0}(\text{quoted})/K, \tag{5.1}$$

where I_{ν_0}(actual) is the actual specific intensity of the sky at frequency ν_0, I_{ν_0}(quoted) is the corresponding value given in a *DIRBE* data product, and ν_0 represents the frequency corresponding to one of the *DIRBE* band nominal wavelengths (1.25, 2.2, 3.5, 4.9, 12, 25, 60, 100, 140, or 240 μm). Thus,

$$K \equiv \frac{\int (I_\nu/I_{\nu_0})_{\mathrm{actual}} R_\nu \mathrm{d}\nu}{\int (\nu_0/\nu)_{\mathrm{quoted}} R_\nu \mathrm{d}\nu} \tag{5.2}$$

where $(I_\nu/I_{\nu_0})_{\mathrm{actual}}$ is the actual specific intensity of the sky normalized to the the intensity at frequency ν_0, and R_ν is the relative system response (see Table A.0-1 in Appendix A). Color correction factors applicable to a variety of source spectral shapes are given in Appendix B and in the ASCII file DIRBE_COLOR_CORRECTION_TABLES.ASC.

5.6 Data Limitations

5.6.1 Photometric and Temporal Discontinuities in the Galactic Plane Maps

The *DIRBE* Galactic Plane Maps contain observations made during the six–month interval from 1990 January 1 to 1990 July 2 inclusive. There are photometric as well as temporal discontinuities in the maps at the two ecliptic longitudes, 10° and 190° (or at Galactic longitudes $\ell \simeq 102°$ and 282°), where the data from January and July meet. The photometric discontinuity is due to the Earth's different orbital positions at those two times and reflects a path difference through the interplanetary dust cloud. The effect is strongest in the spectral region where the zodiacal emission is brightest. Table 5.6-1 gives representative magnitudes of the discontinuities at $\ell \simeq 102°$. The discontinuities are smaller at $\ell \simeq 282$ and are not readily discernible at wavelengths other than those listed.

Table 5.6-1: Photometric discontinuities at $\ell \simeq 102°$

Wavelength (μm)	ΔI_ν MJy/sr
4.9	0.1
12	2.5
25	3.5
60	1.5

5.6.2 Exclusion of Solar System Objects: Gaps in Sky Coverage

In order to avoid contaminating the Weekly Sky Maps with light from moving objects, data obtained when the *DIRBE* pointed near certain solar system objects were excluded when the maps were produced. The "exclusion zones" around these objects were large enough to make their stray light contributions neglibible (see §4.4). The exclusion zones were circles 10° and 1.°5 in radius around the Moon and Jupiter, respectively; around Mars, Uranus, and Neptune, data from 7×7 pixel ($\sim 2.°5 \times 2.°5$) square regions were censored; 3×3 pixel exclusion zones were applied to the asteroids Ceres, Pallas, Vesta, and Juno. Comets Okazaki–Levy–Rudenko (1989R), Austin (1989C1), and Levy (1990C) were extended sources and had exclusion zones as large as 50×50 pixels at 12 and 25 μm (bands 5 and 6) and 20×20 pixels in most other bands during those times when the comets were brightest, and 9×9 pixels at other times. The CIO (or the Time–Ordered Data product) should be consulted for photometric observations of the excluded objects.

Since Saturn, Uranus and Neptune moved slowly across the sky, their exclusion left holes in the Weekly Sky Maps (near the Galactic center on cube face 4). Although faster moving objects, such as the Moon and Mars, did not leave holes in the maps, their locations are often betrayed by discrete patches in which the noise is relatively high because fewer photometric samples were included in the weekly averages.

5.6.3 Extrapolated Values

In the $\varepsilon = 90°$ and Galactic Plane Maps, the quoted intensity values in some pixels were calculated by extrapolation (see §5.2.4). Other pixels observed at ε= 90° at the beginning or end of the cryogenic mission are of lower quality because the baseline available for interpolation is relatively short. A data quality flag identifies the affected data. The FITS headers (see Appendix D) explain how to interpret the data quality flags.

5.6.4 Regions Where the Statistical Noise is Relatively High

Since the photometry errors reported in the Sky Map data products are standard deviations of the mean measured values, any effect that reduces the number of measurements increases the statistical error. Such effects and others that cause noise enhancements in the maps are the following:

Elective exclusion of data – Data deemed to be of low quality were excluded for a variety of reasons (see §4.7). Data deleted for the following reasons led to regions of relatively high noise in the maps:

- observations made while the Moon, planets, or comets (especially the Moon and Jupiter) were in close proximity to the *DIRBE* line of sight
- data obtained while the spacecraft was in the SAA
- unusually noisy 60 μm (band 7) data
- high focal plane temperatures, *e.g.*, caused by Earth rising over the Sun–Earth shield or *FIRAS* calibrations
- data at 4.9 and 60 μm (bands 4 and 7) taken while the *FIRAS* external calibrator was moving

Detectors turned off – Gaps in sky coverage resulted when the 1.25 – 100 μm (band 1 – 8) detectors were turned off for instrument offset testing (see §3.3.2). These gaps gave rise to localized noisy regions in the $\varepsilon = 90°$ Sky Maps. Regions observed at solar elongation angles near 90° during the time intervals 90110–90135 and 90217–90242 were potentially affected.

Uneven depth of sky coverage – As illustrated in Figure 3.1-1(b), the number of observations made per pixel varied over the sky. The depth of coverage is reflected in the photometric noise given in the Annual Average Sky Maps.

Short–term gain fluctuations – Primarily at 12 – 100 μm (bands 5–8), short–term fluctuations in the detector gains (see §4.5.3.1), when not fully corrected, contributed to the dispersion of the photometric measurements and sometimes led to noisy patches in the maps. For example, the effect of residual, uncorrected PIRE at 100 μm is concentrated near the Galactic plane. Also, SAA–induced and IRS–induced gain changes tended to be less well corrected at times when the *COBE* spacecraft was exiting the SAA; the affected regions of the sky in these cases moved slowly as the *DIRBE* viewing swath precessed.

Large brightness gradients – Unresolved sky brightness structures contribute to the dispersion in the photometric measurements averaged in a map pixel because the *DIRBE* beam centroid location and position angle vary from sample to sample. The effect is most severe in parts of the sky that contain strong point sources or brightness gradients.

5.6.5 Negative Intensities at 140 μm and 240 μm

In regions of low signal–to–noise ratio in the 140 and 240 μm maps, some of the quoted pixel intensities are negative. Coaddition of the data obtained over a period of weeks may be required to achieve a positive detection in a faint region at these wavelengths. Some negative pixel intensity values remain in the Annual Average Sky Maps.

5.6.6 Point Source Photometry from the Maps

As a rule, it is recommended that the DIRBE Calibrated Individual Observations (or Time–Ordered Data), not the Sky Maps, be used to determine the fluxes of point sources. Because of the manner in which the sky was scanned and intensity values were assigned to pixels, the "point spread function" applicable to the *DIRBE* Sky Maps is not the same as the beam profile. In particular, the observations averaged to derive a pixel intensity were made at various beam centroid locations (scattered around the nominal pixel center coordinates) and position angles or, equivalently, approach directions. Over a period of months, a typical point source was observed after being approached from a variety of directions, which may or may not have been uniformly distributed over all possible directions. Since over the course of a week the viewing perspective did not change much, point source photometry in the Weekly Sky Maps is particularly susceptible to any bias associated with approach from a limited range of directions. No compensation was made for the point spread functions applicable to individual map pixels because the *DIRBE* maps were intended to provide information about the diffuse sky brightness and not about point sources.

For those who wish to disregard the advice given above and use the *DIRBE* Sky Maps to determine the flux of a point source, it is recommended that the peak pixel intensity in a map rather than an integral over the point spread function be used; a better signal–to–noise ratio will be obtained in this case even if the $\varepsilon = 90°$ Sky Maps, Galactic Plane Maps, or Annual Average Sky Maps, which average over many approach angles, are used. From the peak brightness, subtract an estimate of the background brightness and multiply by the beam solid angle (see Table 4.2-1) to estimate the source flux. The fluxes of bright 2.2 μm sources estimated using peak intensities from the Galactic Plane Maps or the Annual Average Sky Maps were found to be systematically 6 – 9% ($\pm$1% rms) lower than those based upon sightings in the Time–Ordered Data in which the beam crossed the source at the location of peak response. A similar, though smaller (3% $\pm$1% rms), effect was found at 4.9 μm .

5.6.7 Annual Average Sky Maps

Although the Annual Average Sky Maps maximize the signal–to–noise ratio, the Weekly Sky Maps were coadded before the time–dependent zodiacal light component was removed. The variable zodiacal signal, coupled with non–uniform sky coverage, produced spurious features in the Annual Average Sky Maps which are particularly evident at 4.9 – 100 μm (bands 4–8). At wavelengths where the zodiacal emission is weak, the artifacts are less significant and the Annual Average Sky Maps resemble corresponding $\varepsilon = 90°$ Sky Maps. The 140 and 240 μm Annual Average Sky Maps are particularly useful because the zodiacal component is weak at these wavelengths and the signal–to–noise ratio improvement enables detection of otherwise undetectable faint emission at high Galactic latitudes.

5.6.8 4.9 μm Data Excluded from Maps

When the *FIRAS* external calibrator was moved into the *FIRAS* sky horn, the 4.9 μm (band 4) signal exhibited high–frequency (microphonic) noise. Since the noise lasted at most 75 seconds (see §4.7.8), all 4.9 μm data obtained for 75 s following each calibrator move were excluded from the *DIRBE* Sky Maps, though not from the Time–Ordered Data. Table 5.6-2 lists the dates and times when the calibrator was moved.

5.6.9 JFET–off Test Periods

Observations made during the two JFET–off test periods are of limited quality and quantity (see §3.3.2). As noted in Tables 3.1-2 and 5.7-1, the tests were conducted during mission weeks 24, 39, and 40.

5.7 The Project Data Sets

This section gives a detailed description of the contents of each of the *DIRBE* Project Data Sets.

5.7.1 Time–ordered Data

Time–Ordered Data covering the entire cryogenic mission, from 89345 to 90264, are provided in the 41 files listed in Table 5.7-1. Each fixed record length file gives the complete set of data for one week in

Table 5.6-2: *FIRAS* external calibration times

Day Number	Date and Time (UT)
90049	1990 Feb 18 02:38
90079	1990 Mar 20 16:52
90110	1990 Apr 20 19:13
90138	1990 May 18 23:32
90181	1990 Jun 30 13:48
90220	1990 Aug 8 05:54
90229	1990 Aug 17 13:58
90234	1990 Aug 22 14:40
90239	1990 Aug 27 16:22
90244	1990 Sep 1 13:40
90248	1990 Sep 5 15:56
90253	1990 Sep 10 22:54
90257	1990 Sep 14 10:35
90262	1990 Sep 19 10:16

its native VAX binary format. The record length is 10240 bytes. Each record contains the data for a 32–second *DIRBE* "Major Frame."

In the normal Science Data Mode (SDM; see §2.2.6), each of the 16 *DIRBE* detectors was sampled at $\frac{1}{8}$–second intervals, yielding 256 samples per detector per Major Frame. The SDM Time–Ordered photometric data were calibrated using the same algorithms as those applied to the sky map data and are given in units of MJy/sr. However, not all of the Time–Ordered Data records represent nominal SDM skyward–looking data: data obtained in the various calibration modes (see §2.2.6) and during special test periods (see §3.3.2) are included as well; these records are uncalibrated and essentially in their original telemetry form. Pointing information is stored in each record as an array of attitude quaternions, the usage of which is described in §5.7.1.2. There is also a great deal of ancillary spacecraft, environmental and operational information in each record.

Refer to Table 3.1-2 for a summary of weekly sky coverage, and the *DIRBE* Cold Mission Events Log (Appendix C) for a chronological record of non–survey mode activities. Table 5.7-2 summarizes the key fields present in each Time–Ordered Data record. The record contents are described in greater detail in an ASCII file called `DIRBE_TOD_RECORD_STRUCTURE.ASC`.

5.7.1.1 Time Convention

In the Time–Ordered Data and other *DIRBE* data products, time ($T81$) is given in International Atomic Time (TAI) seconds since 1981 January 1 00:00:00 UTC. The 1981.0 fiducial point was adopted to facilitate comparison of the *DIRBE* data with the *IRAS* Zodiacal Observation History File. As a reference point, $T81 = 283996806.0000$ at 1990 January 1 00:00:00 UTC.

5.7.1.2 Using Quaternions

Quaternions, which allow the spacecraft attitude information to be stored compactly (Wertz 1978, Appendix D), can be translated into more familiar coordinates as follows:

Associate a quaternion value with each of the 256 observations in the Major Frame. While the detector data were stored every $\frac{1}{8}$th of a second (at half minor frame intervals), the 4–component quaternions were stored only every 4 seconds. The time associated with the first quaternion is the Major frame time (T81) minus 0.3125 s. The quaternion components should be individually interpolated to the half minor frame times. A cubic spline fit through two preceding and two succeeding quaternions was employed for this purpose in the *DIRBE* processing software.

Table 5.7-1: Time–Ordered Data files

File	Week	Time interval (yyddd)	File name suffix[a]	Start time[b]	Stop time[b]	Records
1	4	89345 – 89351	961081620	282182409.549	282787209.549	18721
2	5	89352 – 89358	961081630	282787209.549	283392009.549	18732
3	6	89359 – 89365	961081640	283392009.549	283996809.549	18749
4	7	90001 – 90007	961091019	283996809.549	284601609.554	18742
5	8	90008 – 90014	961091029	284601609.554	285206409.554	18762
6	9	90015 – 90021	961091039	285206409.554	285811209.554	18723
7	10	90022 – 90028	961091048	285811209.554	286416009.554	18594
8	11	90029 – 90035	961091058	286416009.554	287020809.554	18750
9	12	90036 – 90042	961091108	287020809.554	287625609.558	18759
10	13	90043 – 90049	961091117	287625609.558	288230409.560	18759
11	14	90050 – 90056	961091127	288230409.560	288835209.577	18700
12	15	90057 – 90063	961101651	288835209.577	289440009.581	18720
13	16	90064 – 90070	961101700	289440009.581	290044809.585	18737
14	17	90071 – 90077	961101710	290044809.585	290649609.587	18750
15	18	90078 – 90084	961101719	290649609.587	291254409.589	18713
16	19	90085 – 90091	961101728	291254409.589	291859209.589	18744
17	20	90092 – 90098	961101738	291859209.589	292464009.587	18755
18	21	90099 – 90105	961101747	292464009.587	293068809.585	18733
19	22	90106 – 90112	961101756	293068809.585	293673609.585	18754
20	23	90113 – 90119	961101806	293673609.585	294278409.585	18712
21	24	90120 – 90126[c]	961101815	294278409.585	294883209.588	18734
22	25	90127 – 90133	961101823	294883209.588	295488009.597	18748
23	26	90134 – 90140	961101833	295488009.597	296092809.599	18704
24	27	90141 – 90147	961141119	296092809.599	296697609.607	18676
25	28	90148 – 90154	961141129	296697609.607	297302409.611	18770
26	29	90155 – 90161	961141139	297302409.611	297907209.622	18755
27	30	90162 – 90168	961141148	297907209.622	298512009.626	18537
28	31	90169 – 90175	961141158	298512009.626	299116809.623	18668
29	32	90176 – 90182	961151326	299116809.623	299721609.620	18673
30	33	90183 – 90189	961151335	299721609.620	300326409.620	18719
31	34	90190 – 90196	961151344	300326409.620	300931209.620	18760
32	35	90197 – 90203	961151353	300931209.620	301536009.626	18725
33	36	90204 – 90210	961151402	301536009.626	302140809.626	18690
34	37	90211 – 90217	961151412	302140809.626	302745609.635	18748
35	38	90218 – 90224	961151421	302745609.635	303350409.635	18724
36	39	90225 – 90231[c]	961151430	303350409.635	303955209.645	18591
37	40	90232 – 90238[c]	961151439	303955209.645	304560009.648	18719
38	41	90239 – 90245	961151448	304560009.648	305164809.655	18606
39	42	90246 – 90252	961151457	305164809.655	305769609.661	18755
40	43	90253 – 90259	961151506	305769609.661	306374409.667	18756
41	44	90260 – 90264	961151515	306374409.667	306754537.671	11782

[a] File names are of the form BPC_DTOCI.CAL_INTNS_*nnnnnnnnn*, where *nnnnnnnnn* is the tabulated suffix.
[b] $T81$ (see §5.7.1.1).
[c] Coverage reduced due to JFET–off test.

Table 5.7-2: Key fields in the Time–Ordered Data record

<table>
<tr><th>Name</th><th>First Byte</th><th>Description</th></tr>
<tr><td>ATT_QUAT</td><td>108</td><td>the 4–component attitude quaternions (best available solution) corresponding to eight 4–second intervals starting at the middle of the first "half minor frame."[a] Each quaternion component is a 32–bit floating point number.</td></tr>
<tr><td>T81_time</td><td>245</td><td>64–bit floating point Major Frame start time in International Atomic Time (TAI) seconds since 1981 January 1 00:00:00 UTC. The time in the middle of the first half minor frame is T81_time − 0.3125 s.</td></tr>
<tr><td>DADRBSCI2</td><td>512</td><td>Calibrated detector data in an array corresponding to 16 detectors × 256 half minor frame samples, in the detector sampling order specified by DAMEPS (see below). Each datum is compressed into a signed 2–byte integer with the following bit structure:

(MSB) s n n n n x x x x x x x x x x x (LSB)

One of two formulas must be used to reconstruct values, R, in MJy/sr. If DADRBSCI2 is positive (i.e., s is set to 0), then $R = X2^N M/f(b)$, where X is the integer represented by bits 0 – 10 (the x's), N is the integer represented by bits 11 – 14 (the n's), M is the smallest detectable non–zero signal (0.5) at maximum gain (16 × 27.12; i.e., $M = 0.5/(16 \times 27.12)$, and $f(b)$ is the applicable wavelength band–dependent scale factor from the table below. If DADRBSCI2 is negative (i.e., s is set to 1) and has a value greater than or equal to -28358, take the absolute value,[b] extract the N and X (15 least significant) bits, and then calculate $R = -X2^N M/f(b)$.

<table>
<tr><th>b</th><th>f(b)</th></tr>
<tr><td>1A</td><td>3.0</td></tr>
<tr><td>1B</td><td>2.4</td></tr>
<tr><td>1C</td><td>1.9</td></tr>
<tr><td>2A</td><td>2.6</td></tr>
<tr><td>2B</td><td>0.86</td></tr>
<tr><td>2C</td><td>0.74</td></tr>
<tr><td>3A</td><td>3.2</td></tr>
<tr><td>3B</td><td>1.1</td></tr>
<tr><td>3C</td><td>0.90</td></tr>
<tr><td>4</td><td>3.1</td></tr>
<tr><td>5</td><td>0.88</td></tr>
<tr><td>6</td><td>0.64</td></tr>
<tr><td>7</td><td>0.20</td></tr>
<tr><td>8</td><td>0.29</td></tr>
<tr><td>9</td><td>0.013</td></tr>
<tr><td>10</td><td>0.026</td></tr>
</table>

The roundoff error associated with compression and reconstruction is less than or equal to 0.05% (1σ) or $0.0006/f(b)$ MJy/sr, whichever is greater.

DADRBSCI2 values less than -28358 are given when the data have no scientific utility. One may add 11985 to such values and interpret them as described in Table 4.7-1.</td></tr>
</table>

<table>
<tr>
<td><code>DAMEPS</code></td>
<td>9232</td>
<td>32–byte array giving the detector sampling order for the previous Major Frame. The bytes at array positions $2N-1$ and $2N$, where $N = 1, 2, \ldots, 16$, correspond, respectively, to the high ($\times 16$) and low ($\times 1$) gain (see §2.2.5)MUX entry port addresses for the Nth process sampled by the MUX. The byte values are related to detector numbers as follows:
<table>
<tr><th>Band</th><th>Byte $2N-1$ (high gain)</th><th>Byte $2N$ (low gain)</th></tr>
<tr><td>1A</td><td>16</td><td>0</td></tr>
<tr><td>2A</td><td>17</td><td>1</td></tr>
<tr><td>3A</td><td>18</td><td>2</td></tr>
<tr><td>1B</td><td>19</td><td>3</td></tr>
<tr><td>2B</td><td>20</td><td>4</td></tr>
<tr><td>3B</td><td>21</td><td>5</td></tr>
<tr><td>1C</td><td>22</td><td>6</td></tr>
<tr><td>2C</td><td>23</td><td>7</td></tr>
<tr><td>3C</td><td>24</td><td>8</td></tr>
<tr><td>4</td><td>25</td><td>9</td></tr>
<tr><td>5</td><td>26</td><td>10</td></tr>
<tr><td>6</td><td>27</td><td>11</td></tr>
<tr><td>7</td><td>28</td><td>12</td></tr>
<tr><td>8</td><td>29</td><td>13</td></tr>
<tr><td>9</td><td>30</td><td>14</td></tr>
<tr><td>10</td><td>31</td><td>15</td></tr>
</table>
For example, <code>DADBRSCI2</code> values $(N, 1:256)$ where $N = 1$ correspond to MUX process 1. Thus, if bytes $2N-1$ $(=1)$ and $2N$ $(=2)$ have values of 23 and 7, respectively, then the table above shows that the first 256 <code>DADBRSCI2</code> values refer to data from detector 2C. A similar algorithm can be used to assign detector numbers to each of the 16 processes for which detector data are given in <code>DADBRSCI2</code>.</td>
</tr>
<tr>
<td><code>PCSV</code></td>
<td>9512</td>
<td>an 8–byte array, called the "Pipeline Compressed State Vector," of which only the second byte will be useful in most research applications. Byte 2 indicates "external" factors that influence the data quality and should be interpreted as follows:
<table>
<tr><th>External factor (Bits)</th><th>Value</th><th>Interpretation</th></tr>
<tr><td>Fill data flag (0–1)</td><td>01
11</td><td>some minor frames missing
all minor frames missing</td></tr>
<tr><td>Attitude control (2–3)</td><td>01
10</td><td>spacecraft slewing
special pointing</td></tr>
<tr><td>Attitude solution (4–5)</td><td>11
10
00</td><td>coarse aspect (non–definitive)
coarse aspect (definitive)
DIRBE fine aspect (definitive)</td></tr>
<tr><td>COBE location† (6–7)</td><td>00
01
10
11</td><td>okay (or not checked, for backward compatibility)
in NVAB horn
in SVAB horn
in the SAA</td></tr>
</table>
† location relative to SAA and radiation belts 16 seconds after the Major Frame start time. Data when the spacecraft was in the SAA were of suspect quality and should not be used for scientific investigations.</td>
</tr>
</table>

`DAOMS`	9623	operating mode for the Major Frame encoded in a single byte. 0 ⇒ Science Data Mode (SDM). *Always check this field before decoding the data.*

[a] the 32–second Major Frame is divided into 128 minor frames (or 256 half minor frames), each lasting 0.25 s. In SDM, each detector's output was sampled once per half minor frame (*i.e.*, at $\frac{1}{8}$–second intervals).

[b] This assumes that twos complement representation is used for integers, as is the case on a VAX/VMS machine such as the one used to prepare the data product.

Construct a matrix of the following form:

$$\boldsymbol{A} = \begin{pmatrix} Q_{44}+Q_{11}-Q_{22}-Q_{33} & 2(Q_{12}-Q_{34}) & 2(Q_{13}+Q_{24}) \\ 2(Q_{12}+Q_{34}) & Q_{44}-Q_{11}+Q_{22}-Q_{33} & 2(Q_{23}-Q_{14}) \\ 2(Q_{13}-Q_{24}) & 2(Q_{23}+Q_{14}) & Q_{44}-Q_{11}-Q_{22}+Q_{33} \end{pmatrix}$$

where $Q_{ij} = q_i q_j$ and (q_1, q_2, q_3, q_4) is the quaternion. (The quaternion components appear in order from q_1 first to q_4 last in the Time–Ordered Data files.)

Matrix $\boldsymbol{A}$ enables transformation from coordinates fixed in the spacecraft reference frame to epoch 2000.0 geocentric equatorial coordinates.

Transform the *DIRBE* boresight vector coordinates to equatorial coordinates. The boresight vector in spacecraft coordinates is

$$\boldsymbol{V} = \begin{pmatrix} -0.86708729 \\ 0.43196023 \\ -0.24813300 \end{pmatrix}.$$

Thus the instantaneous *DIRBE* line of sight coordinates, $\boldsymbol{D} = \boldsymbol{AV}$. $\boldsymbol{D}$ is related to epoch 2000 Right Ascension (RA) and Declination (DEC) as follows:

$$\boldsymbol{D} = \begin{pmatrix} \cos RA \cos DEC \\ \sin RA \cos DEC \\ \sin DEC \end{pmatrix},$$

where RA and DEC are in radians.

5.7.1.3 Standard MUX Sequence

During routine operations, the *DIRBE* detectors were sampled in the order specified in the second column of Table 3.2-1. Users of the Time–Ordered Data should check their decoding results for the DAMEPS field against the standard sequence. One should obtain the standard MUX sequence in most cases.

5.7.1.4 Notes on the Use of Polarization Data in the TOD

The intensities in the polarization and photometry channels are all independently celestially stabilized in the same fashion. To preserve the values of the ratios of the intensities in the 'B' and 'C' channels relative to the photometric ('A') channels, the absolute calibration applied to the polarization data in the TOD is handled differently than that of the photometry: the calibration factors and beam solid angles are fixed to the same values used for the corresponding photometric channels.

To calculate the polarizations in the 'B' and 'C' channels, the measured intensities in each channel are iteratively fitted to an expression of the form:

$$S_{\lambda,B \text{ or } C} = Q\cos 2\Theta + U \sin 2\Theta \tag{5.3}$$

where

$$S_{\lambda,B} = 1 - \frac{(I_{\lambda,B}/I_{\lambda,A})\,(\Omega_{\lambda,A}/\Omega_{\lambda,B})}{K_{\lambda,B}},$$

$$S_{\lambda,C} = \frac{(I_{\lambda,C}/I_{\lambda,A})\,(\Omega_{\lambda,A}/\Omega_{\lambda,C})}{K_{\lambda,C}} - 1,$$

$K_{\lambda,B}$ and $K_{\lambda,C}$ are the polarization coefficients listed in Table 5.7-3, and Ω is the beam solid angle (see Table 4.2-1).

Table 5.7-3: Polarization coefficients

λ (μm)	$K_{\lambda,B}$	$\sigma^a_{K_{\lambda,B}}$	$K_{\lambda,C}$	$\sigma^a_{K_{\lambda,C}}$
1.25	0.784	0.002	0.630	0.002
2.2	0.359	0.002	0.303	0.002
3.5	0.317	0.002	0.279	0.002

[a] standard deviation of the mean

The quantity $S_{\lambda,B \text{ or } C}$ is the fractional signal in the 'B' or 'C' channel relative to 'A', after both channels are placed on the same relative photometric scale via the scaling factors $K_{\lambda,B \text{ or } C}$ $(\Omega_{\lambda,B \text{ or } C}/\Omega_{\lambda,A})$. The polarization coefficients, K, are derived from observations of unpolarized point sources corrected for channel–to–channel differences in detector responsivity. The solid angle ratio $(\Omega_{\lambda,B \text{ or } C}/\Omega_{\lambda,A})$ compensates for variations in the beam profile.

To compute the Stokes parameters Q and U from the 'B' and 'C' channel intensities, the orientations of the polarizers, Θ, must be known, but polarizer orientations are not provided in the TOD. The orientations must be calculated from the time of observation via the attitude solution and spacecraft angular velocity, both of which are provided.

5.7.2 Calibrated Individual Observations and Associated Pixel Index Files

The Calibrated Individual Observations (CIO) files tabulate the calibrated individual $\frac{1}{8}$th–second sky survey data samples taken during each day of the cryogenic mission. The CIO files are much more convenient to use than the TOD product, and, in nearly all applications, can be substituted for the TOD. Relative to the TOD, the CIO files

- contain only science survey–mode data;
- omit selected low–quality data;
- present the data in wavelength band, rather than MUX–sequence, order;
- give pointing information in terms of pixel numbers instead of attitude quaternions; and
- are in standard FITS, rather than native (VAX) binary format.

The CIO database is organized into 285 pairs of files, one pair per day, where a "pair" consists of a data file and its associated pixel index file. The data pertaining to observations made between 0h UT and 23:59:59.999 UT, inclusive, are given in a single data file. Within each daily file, the observations are arranged in order of ascending *DIRBE* pixel number, and, whenever a given pixel is observed multiple times, the data for that pixel are given in chronological order.

The Pixel Index files are also organized in ascending pixel number order, and can be used to determine which pixels were observed on a given day. For each pixel, the CIO Pixel Index file lists the number of the last row in the corresponding CIO data file that contains information on that pixel. The number of the *first* row containing data on a given pixel can be derived by adding 1 to the `LastRow` value tabulated in the previous record; data pertaining to the first pixel listed in the Index table begins in row 1 of the data table.

For example, the first four entries in the Pixel Index file for day 89345 indicate that the last CIO data file rows containing data on pixels 20, 21, 22, and 23 are 6, 19, 20, and 30, respectively. According to the algorithm given above, the first rows containing data on these pixels are 1, 7, 20, and 21. In other words, the data pertaining to pixel 20 can be found in rows 1 through 6, the data on pixel 21 in rows 7 through 19, etc.

Tables 5.7-4 and 5.7-5 summarize the contents of the Calibrated Individual Observations and CIO Pixel Index files, respectively. The FITS headers give more detailed information about the individual data fields. Sample CIO and CIO Pixel Index FITS headers are listed in Appendix D. Users of the CIO data products will also need to be familiar with some or all of the information presented in the remainder of this section.

5.7.2.1 Reconstruction of Time Strings

Either one of the following methods could be used to extract a time–ordered data string from a CIO file:

1. ingest an entire day's worth of data, and then sort on the time field; or

2. for a given pixel, use the `Next_obs` (`Prev_obs`) field to locate the table row containing the next (previous) observation in the time sequence, and continue recursively until the desired time string has been selected.

Since non–survey mode and SAA crossing data are removed from the CIO dataset, the observations to which `Next_obs` and `Prev_obs` point are not always separated in time by $\pm\frac{1}{8}$th second from the current observation; gaps exist in the time sequence. Data in the `Time` field can be used to check for gaps.

5.7.2.2 Reconstitution of Attack Vector Values

Attack Vector values, `AttackV`, are represented as two–byte integers in the CIO files. Physical values will be reconstituted by generic FITS–reading software according to a transformation of the form $\text{physical value} = \texttt{TSCAL} \times \text{stored value} + \texttt{TZERO}$. In the FITS files, `TSCAL` is assigned the value 2^{-15}, and `TZERO` is set to 0.

An offset *not* taken into account by `TZERO` should be added to the reconstituted `AttackV` values to compensate for a bug in the software used to calculate the integers recorded in the FITS files. Table 5.7-6 indicates how the offset should be applied. The correction will be applied automatically by the *COBE* analysis software (see §D.1; version 3.0 or higher).

5.7.2.3 Determination of Sky Coordinates

The tabulated `Pixel_no` corresponds to a position within the boundary of a resolution 9 ($0\overset{\circ}{.}32$ square) CSC pixel (see §5.3). More accurate positions can be calculated if one uses the tabulated `PSubPos` and `PSbSbPos` data to reconstruct a resolution 15 quad–sphere "super pixel number," defined as follows:

$$\text{super pixel number} = 4096 \times \texttt{Pixel\_no} + 16 \times \texttt{PSubPos} + \texttt{PSbSbPos}. \tag{5.4}$$

Appendix D.1 lists programs that can be used to compute sky coordinates from input resolution 9 or resolution 15 CSC pixel numbers; a different program is required for each resolution. A resolution 15 pixel is a roughly $20''$ square.

"Super pixel number" positions correspond to the nominal attitude, which was derived from the ensemble of data from all three 2.2 μm detectors. However, as indicated in Table 4.2-1, the beam centroid of each individual detector can be offset by up to a few arcminutes from this nominal position due to differences in the beam profiles. Thus, in order to derive precise sky coordinates, detector–dependent corrections must be applied to the super pixel number coordinates. The correction calculation should go as follows.

1. Convert the super pixel number to an ecliptic J2000 3–vector line of sight (LOS) using the `SUPERCENPIX` routine;

Table 5.7-4: Columns in the Calibrated Individual Observations FITS tables

n	TTYPEn[a]	Description
1	`Pixel_no`	*DIRBE pixel number* (signed 32–bit integer) Pixel number in the CSC projection (see §5.3).
2	`PSubPos`	*Pixel sub–position* (8–bit byte) Location of the line of sight within pixel `Pixel_no`.
3	`PSbSbPos`	*Pixel sub-sub-position* (8–bit byte) Location of the line of sight within sub–pixel `PSubPos`.
4	`Time`	*Time* (64–bit floating point) Time of observation in atomic (TAI) seconds elapsed since 1981 January 1 00:00:00 UTC[b].
5	`Next_obs`	*Pointer to next observation* (32–bit integer) Number of the row in this table containing data on the next observation in the time sequence. Nominally the next survey–mode observation was made at `Time` + $\frac{1}{8}$th sec.
6	`Prev_obs`	*Pointer to previous observation* (32–bit integer) Number of the row in this table containing data on the previous observation in the time sequence. Nominally the preceding survey–mode observation was made at `Time` − $\frac{1}{8}$th sec.
		Intensities, in MJy/sr, reported for a single, $\frac{1}{8}$th second sample: (all 32–bit floating point)
7	`Phot1A`	1.25 μm full (Band 1A) intensity
8	`Phot1B`	1.25 μm polarized light (Band 1B) intensity
9	`Phot1C`	1.25 μm polarized light (Band 1C) intensity
10	`Phot2A`	2.2 μm full (Band 2A) intensity
11	`Phot2B`	2.2 μm polarized light (Band 2B) intensity
12	`Phot2C`	2.2 μm polarized light (Band 2C) intensity
13	`Phot3A`	3.5 μm full (Band 3A) intensity
14	`Phot3B`	3.5 μm polarized light (Band 3B) intensity
15	`Phot3C`	3.5 μm polarized light (Band 3C) intensity
16	`Phot04`	4.9 μm (Band 4) intensity
17	`Phot05`	12 μm (Band 5) intensity
18	`Phot06`	25 μm (Band 6) intensity
19	`Phot07`	60 μm (Band 7) intensity
20	`Phot08`	100 μm (Band 8) intensity
21	`Phot09`	140 μm (Band 9) intensity
22	`Phot10`	240 μm (Band 10) intensity
23	`LOS2VelV`	*Angle between DIRBE line of sight and spacecraft orbital velocity vector* (signed 16–bit integer)
24	`ApprVec`	*Approach Vector* (8–bit byte) Observations were classified as "forward–looking," and assigned Approach Vector value 1, if the line of sight was aligned within 90° of the direction of spacecraft motion; otherwise the observation was "backward–looking" and the Approach Vector was assigned the value 2.
25	`AttackV`	*Attack Vector* (vector of 3 signed 16–bit integers) A vector whose three components specify the rate of change (derivative with respect to time) of the *DIRBE* boresight unit vector.
26	`AtV_Azim`	*Azimuth of the Attack Vector* (signed 16–bit integer) Azimuth relative to a fiducial zero angle defined by the cross product of the *DIRBE* spin axis and boresight vectors.
27	`SolElong`	*Solar elongation angle,* ε (signed 16–bit integer) Angle between the spacecraft–Sun vector and the *DIRBE* line of sight.
28	`Moon2LOS`	*Angle between spacecraft–Moon vector and DIRBE line of sight* (signed 16–bit integer) When `Moon2LOS` $\leqq$ 10 ° the observations are potentially contaminated by lunar stray light.

29	`MoonAzim`	*Azimuth of the Moon* (signed 16–bit integer) Azimuth of the projection of the spacecraft–Moon vector onto the plane normal to the *DIRBE* line of sight relative to the fiducial zero angle defined above (see description of `AtV_Azim`).
30	`Jup2LOS`	*Angle between spacecraft–Jupiter vector and DIRBE line of sight* (signed 16–bit integer) When `Jup2LOS` $\leqq 1\overset{\circ}{.}5$ the observations are potentially contaminated by stray light from Jupiter.
31	`RadZone`	*Radiation zone flag* (8–bit byte) Flag indicates if the spacecraft was within the South Atlantic Anomaly (SAA), North Van Allen Belt (NVAB) or South Van Allen Belt (SVAB) at the time of observation.
32	`XSNoise`	*Excess noise flag* (signed 16–bit integer) Flags indicate whether exceptionally noisy data were recorded during the 32–second long Major Frame that included this observation. Each of the 16 bits corresponds to one *DIRBE* detector.
33	`OA_Flags`	*Orbit and attitude flags* (8–bit byte) Miscellaneous orbit and attitude information.

[a] FITS keyword giving the label or heading for field (*i.e.*, table column) `n`.
[b] $T81$ (see §5.7.1.1).

Table 5.7-5: Columns in the CIO Pixel Index FITS tables

`n`	`TTYPEn`[a]	Description
1	`Pixel_no`	*DIRBE pixel number* (signed 32–bit integer) Pixel number in the CSC projection.
2	`LastRow`	*Last row number* (signed 32–bit integer) Number of the last row in the corresponding CIO data table that contains data on this pixel.

[a] FITS keyword giving the label or heading for field (*i.e.*, table column) `n`.

Table 5.7-6: Offset corrections for Attack Vectors in CIO files

If the physical value `AttackV`×`TSCAL`[a] is	Then add
value $\geqq$ `TSCAL`	$0.5 \times$ `TSCAL`
value $\leqq$ $-$`TSCAL`	$-0.5 \times$ `TSCAL`
0.0	0.0

[a] $\mathtt{TSCAL} = 2^{-15}$

2. look up (or read from the ASCII file `DIRBE_BEAM_CHARACTERISTICS_P3B.ASC`) the in–scan and cross–scan beam centroid offsets corresponding to the detector of interest, and convert them to units of radians;

3. normalize the tabulated Attack Vector data (`AttackV`) by dividing each component by the magnitude,
$$\sqrt{\mathtt{AttackV}(1)^2 + \mathtt{AttackV}(2)^2 + \mathtt{AttackV}(3)^2},$$
and call the normalized vector NATV; and

4. calculate the components of the new line of sight vector, LOS′, as follows:

$$\mathrm{LOS}'(1) = \mathrm{LOS}(1) + \mathrm{ISCO} \times \mathrm{NATV}(1) + \mathrm{XSCO} \times [\mathrm{LOS}(2) \times \mathrm{NATV}(3) - \mathrm{LOS}(3) \times \mathrm{NATV}(2)]\,,$$

$$\mathrm{LOS}'(2) = \mathrm{LOS}(2) + \mathrm{ISCO} \times \mathrm{NATV}(2) + \mathrm{XSCO} \times [\mathrm{LOS}(3) \times \mathrm{NATV}(1) - \mathrm{LOS}(1) \times \mathrm{NATV}(3)]\,,$$

and

$$\mathrm{LOS}'(3) = \mathrm{LOS}(3) + \mathrm{ISCO} \times \mathrm{NATV}(3) + \mathrm{XSCO} \times [\mathrm{LOS}(1) \times \mathrm{NATV}(2) - \mathrm{LOS}(2) \times \mathrm{NATV}(1)]\,,$$

where ISCO and XSCO are the in–scan and cross–scan beam offsets, respectively. The components of LOS′ are direction cosines, in ecliptic J2000 coordinates, corresponding to the centers of the individual detector beams.

Users of the polarization data are advised to apply the ‘A’ channel centroid offsets to the ‘A’,‘B’ and ‘C’ channels when making polarization maps. Failure to do this could lead to incorrect B/A and C/A intensity ratios.

Bear in mind that the *DIRBE* attitude solution has a 1σ uncertainty of $1'.5$. As a rule, in the absence of independent information, it would be *inappropriate to quote positions to greater than arcminute precision.*

5.7.2.4 Quality Flags

Individual observations that failed to pass certain quality tests are replaced in the CIO files by sentinel values $\leqq -16385$. However, some data known to be of low quality, such as observations affected by stray light from the Moon or Jupiter, were not explicitly flagged. Information given in the fields `Moon2LOS` and `Jup2LOS` can be used to cull out unflagged but low–quality data. Data rejection is recommended whenever (a) `Moon2LOS`$\leqq 10°$, (b) `Jup2LOS`$\leqq 1°.5$, or (c) the `XSNoise` flag is set for the detector of interest. Even if the CIO data are filtered as suggested, a few anomalies will remain, especially in Bands 7 and 8 (60 and 100 μm).

5.7.2.5 Polarization Data in the CIO Files

The information in §5.7.1.4 on *Polarization Data in the TOD* also pertains to the CIO, with the exception that the polarizer orientation can be readily calculated from the Attack Vector and pixel number data provided in the CIO.

To compute the Stokes parameters Q and U from the ‘B’ and ‘C’ channel intensities using equation (5.3), the orientations of the ‘C’ channel polarizers, Θ, must be known. By *DIRBE* convention, Θ is defined as the angle between the polarizer axes and the local meridian (*i.e.,* a great circle drawn through the spacecraft and the North and South ecliptic poles). Noting that the transmission axes of the ‘C’ channel polarizers are aligned with the direction of scan motion, Θ can be calculated as follows:

1. Compute the ecliptic longitude and latitude, (λ, β), in radians, from the pixel number, `Pixel_no` (see §5.3)

2. Calculate
$$\mathtt{att\_x} = \mathtt{AttackV}(1)\cos(\lambda) + \mathtt{AttackV}(2)\sin(\lambda)\,,$$
$$\mathtt{att\_y} = \mathtt{AttackV}(2)\cos(\lambda) - \mathtt{AttackV}(1)\sin(\lambda)\,,$$

$$\texttt{colatitude} = \frac{\pi}{2} - \beta,$$

and

$$x' = \texttt{att\_x} \cos(\texttt{colatitude}) - \texttt{AttackV}(3) \sin(\texttt{colatitude})$$

3. Finally, calculate

$$\Theta = \arctan(\texttt{atty}/x'),$$

such that Θ is in the range $[-90°, +90°]$.

Close to the solar elongation extrema, $\varepsilon = 64°$ and $124°$, the 'C' channel transmission axis is nearly aligned with the local meridian, and $\Theta \simeq 0$. When $\varepsilon \sim 94°$, the scan direction is perpendicular to the local meridian and $\Theta \simeq \pm 90°$.

Further information about the *DIRBE* polarization algorithm can be found in Chapter 4. For a summary of polarization results, see Berriman *et al.* (1994).

5.7.3 Weekly Sky Maps

The Weekly Sky Maps give weekly–averaged intensity values for the 10 *DIRBE* photometric bands, plus the Stokes Q and U parameters at 1.25, 2.2 and 3.5 μm. There are 41 Weekly Sky Map files, one per week of optimized operation in the cryogenic mission (see Table 3.1-2).

The files are FITS binary tables. Each table row corresponds to a *DIRBE* pixel. Table 5.7-7 describes the FITS table columns. More complete documentation is provided in the FITS headers (see Appendix D for a sample header listing).

The following two sections are relevant only to the (obsolete) Pass 2B versions of the Weekly Sky Maps. In the Pass 3B versions, non–zero FITS `TZERO` keywords are included in the `DeltaT` and `SolElong` fields to align the data properly with respect to the $\Delta\,Time$ and ε bins, and to allow for negative $\Delta\,Time$ values. Standard FITS ingest software should correctly interpret the Pass 3B data files.

5.7.3.1 Note on Reconstitution of $\Delta\,Time$ Values (Pass 2B only)

The $\Delta\,Time$ field is unique in that it must be interpreted as a scaled signed byte (*i.e.,* as a number in the range -128 to $+127$ linearly transformed into a value of $\Delta\,Time$). Unfortunately, because the FITS standard accomodates only *un*signed bytes (which have values ranging from 0 to 255), generic FITS–reading software will not interpret the $\Delta\,Time$ values properly. Compliance with the FITS standard was intended and an alternate encoding scheme may be applied if new versions of the Weekly Sky Maps are produced. In the meantime the *COBE* analysis software mentioned in §D.1 (version 3.0 or higher) will correctly unpack the $\Delta\,Time$ field. The FORTRAN program `dirbe_wk_read` included in Appendix D illustrates how the data should be treated.

Additional information about the $\Delta\,Time$ field is given below.

Table 5.7-7: Columns in the Weekly Sky Map FITS tables

n	TTYPEn[a]	Description
1	`Pixel_no`	*DIRBE pixel number* (signed 32–bit integer) Pixel number in the CSC projection (see §5.3).
2	`PSubPos`	*Pixel sub–position* (byte) Gives the small but potential offset between the centroid position of the samples included in the weekly average and the pixel center coordinates (see §5.3).
3	`Displace`	*Displacement means* (vector of 4 bytes) The centroid position given by `Pixel_no` and `PSubPos` is based upon the attitude solution, and thus upon band 2 (2.2 μm; see §4.3). Although the *DIRBE* map–making software compensates for the relative locations of the beams associated with the other bands (see §4.2.2), `PSubPos` is technically applicable only to band 2. `Displace` gives offsets analogous to `PSubPos` for the four bands that have the greatest beam offsets.
4	`Time`	*Time* (64–bit floating point) Average of the times at which the pixel was observed during the week given in International Atomic Time (TAI) seconds elapsed since 1981 January 1 00:00:00 UTC[b].
5	`DeltaT`	Δ*Time* (vector of 10 bytes) Since the number of measurements included in a weekly average was photometric band–dependent, the `Time` value is only an approximation to the average time the pixel was observed at a particular wavelength. A more accurate time for each band is `Time` plus the value of `DeltaT` for that band.
6	`SolElong`	*Solar elongation angle,* ε (signed 16–bit integer) Average of the solar elongation angles at which the pixel was observed during the week. The comment made about the accuracy of `Time` under `DeltaT` also applies to `SolElong`.
7	`Photomet`	*Photometry* (vector of 10 32–bit floating point values) Average intensity observed for the pixel over the week, in units of MJy/sr. The 10 values correspond to the 10 *DIRBE* bands in order of increasing wavelength.
8	`Stokes`	*Stokes parameters* (vector of 6 32–bit floating point values) Stokes Q and U parameters given as (Q,U) pairs for wavelengths in the order 1.25, 2.2 and 3.5 μm. The Stokes parameters for each band are averages of the individual Qs and Us, weighted according to their uncertainties. Since more stringent data selection criteria were used for the polarimetry than for the photometry, average fields such as `Time`, `DeltaT`, and `SolElong` do not strictly apply to the polarization fields. However, because the Stokes parameters vary only weakly with time and ε, the quoted weekly–averaged values may be assumed to apply.
9	`NumRecs`	*Number of records* (signed 16–bit integer) Number of times the pixel was observed this week in at least one photometric band. (Observations made contemporaneously at multiple wavelengths count once.)
10	`WtNumObs`	*Weighted number of observations* (vector of 10 bytes) Effective number of observations contributing to the weekly averaged intensities (*i.e.*, sum of the weights assigned to the individual measurements). The band–dependent values are given in order of increasing wavelength.

11	`StdDev`	*Photometry standard deviation* (vector of 10 bytes) Standard deviations of the mean intensities for the 10 *DIRBE* bands given in ascending wavelength order and encoded. The FITS header describes how to decode the stored values.
12	`StokesSD`	*Stokes parameter standard deviations* (vector of 6 bytes) Standard deviations of the mean Stokes parameter values given in the same order as the Stokes parameters and encoded. The FITS header describes how to decode the stored values.
13	`SSOFlag`	*Solar system object flag* (byte) Indicates which solar system object exclusion zones (see §5.6.2), if any, intersect the pixel at some time during the week. See FITS header for interpretation instructions.
14	`FracUsed`	*Fraction of data used* (vector of 3 bytes) Percentage of available data used to calculate the weekly average values in all intensity bands, band 1B (1.25 μm), and band 7 (60 μm), respectively.
15	`StokQual`	*Stokes parameter quality flag* (vector of 6 bytes) Set of flags, one per Stokes parameter, indicating factors that affect the quality of the quoted values. See FITS header for interpretation instructions.

[a] FITS keyword giving the label or heading for field (*i.e.*, table column) `n`.
[b] $T81$ (see §5.7.1.1).

5.7.3.2 Note on Reconstitution of "Binned" Quantities (Pass 2B only)

As a space–saving measure $\Delta\,Time$ and mean ε values are not given to full precision in the Weekly Sky Maps. In particular, to represent a $\Delta\,Time$ value in a single byte, the true value was assigned to one of 128 bins, each lasting 4725 seconds (one week divided by 128); analogously, to cast a solar elongation value into a two–byte integer, the true value was assigned to one of 32767 bins, each about a hundredth of a degree wide.

Generic FITS–reading software is supposed to apply a transformation of the form physical value = `TSCAL` × stored value + `TZERO`, where `TSCAL` and `TZERO` come from the FITS header. Values of 0 were mistakenly assigned to `TZERO` for the `DeltaT` and `SolElong` fields; the values that *should* have been assigned, which correspond to half the respective bin intervals, are given in Table 5.7-8. The *COBE* analysis software (see §D.1; version 3.0 or higher) compensates for the error in the data files by adding the tabulated offset values. The FORTRAN program `dirbe_wk_read` included in Appendix D illustrates how the data should be treated.

Table 5.7-8: Offset values for Weekly Sky Map fields

Field	Offset
`DeltaT`	0.5×4725 sec
`SolElong`	$0.5 \times \left[360/\left(2^{15}-1\right)\right]$ deg

5.7.4 *DIRBE* Calibrated Annual File and Associated Pixel Index File

The *DIRBE* Calibrated Annual File (DCAF) is a reorganized form of the Weekly Sky Maps designed to facilitate access to the weekly–averaged intensities seen in individual pixels as a function of time. Those who wish to study or model time–variable signals, such as zodiacal light, will find this organization convenient.

The columns of the DCAF FITS binary table are exactly the same as those in the Weekly Sky Maps (see Table 5.7-7). The rows are organized differently, however. Whereas the Weekly Sky Maps contain only one weekly–averaged row entry per pixel, the DCAF contains multiple row entries per pixel, each corresponding to a week of the cryogenic mission. As in the Weekly Maps, the data are given in ascending *DIRBE* pixel number order; the DCAF data for individual pixels are given in chronological order.

Because of its relatively large size, the DCAF dataset is presented in six files, one for each of the six faces of the *COBE* sky cube. Figures 5.3-1 and 5.3-2 show the relationships between pixel numbers, Galactic coordinates, and cube faces. Table 5.7-9 gives the range of ecliptic coordinates covered by each cube face. The *DIRBE* sky scan strategy (see §2.3.4) was such that pixels above $|\beta| \sim 60°$ were typically observed during each week of the mission, while pixels closer to the ecliptic plane were typically seen during only about half of the mission. Thus, the FACE0 and FACE5 DCAF files are about twice as large as the others.

Table 5.7-9: Ecliptic coordinate ranges covered by CSC cube faces

Cube face number	Range of Pixel numbers	Ecliptic longitude (°)[a]	Ecliptic latitude (°)[a]
0	0 – 65535	0 – 360	+45 – +90
1	65536 – 131071	315 – 45	−45 – +45
2	131072 – 196607	45 – 135	−45 – +45
3	196608 – 262143	135 – 225	−45 – +45
4	262144 – 327679	225 – 315	−45 – +45
5	327680 – 393215	0 – 360	−45 – −90

[a] The ecliptic coordinate ranges are approximate.

A separate DCAF Pixel Index table is provided for each cube face. Table 5.7-10 lists the fields in a DCAF index table. One can use the tabulated `LastRow` to determine which rows (*i.e.,* range of row numbers) in the corresponding DCAF data file contain data on a specific pixel. To calculate "`FirstRow`," the number of the first row in the range, add 1 to the `LastRow` value listed for the previous pixel; for the first listed pixel, "`FirstRow`" is equal to 1. (This calculation is illustrated in an example given in §5.7.2.) Once a range of row numbers has been specified, a FITS reader can be used to extract only the desired data, thus expediting data selection.

Sample DCAF and DCAF Pixel Index FITS headers are listed in Appendix D. The FITS headers give more detailed information about the individual data fields.

Table 5.7-10: Columns in the DCAF Pixel Index FITS tables

n	TTYPEn[a]	Description
1	`Pixel_no`	*DIRBE pixel number* (signed 32–bit integer) Pixel number in the CSC projection.
2	`LastRow`	*Last row number* (signed 32–bit integer) Number of the last row in the corresponding DCAF data table that contains data on this pixel.
3	`WksObs`	*Weeks observed flag* (6 8–bit byte) Each bit set to 1 corresponds to a week during the cryogenic mission when the pixel was observed.

[a] FITS keyword giving the label or heading for field (*i.e.*, table column) `n`.

5.7.5 $\varepsilon = 90°$ Sky Maps

The $\varepsilon = 90°$ Sky Maps are provided in 10 FITS binary table files, one per *DIRBE* intensity band. Both the file names and the FITS headers indicate to which band the data apply. Each row of the FITS table corresponds to a *DIRBE* pixel. However, for reasons described in §5.2.6, there are sometimes two entries, and hence two table rows, for a pixel. Table 5.7-11 describes the FITS table columns. More complete documentation is provided in the FITS headers (see Appendix D for a sample header listing).

Table 5.7-11: Columns in the $\varepsilon = 90°$ Sky Map FITS tables

n	TTYPEn[a]	Description
1	`Pixel_no`	*DIRBE pixel number* (signed 32–bit integer) Pixel number in the CSC projection (see §5.3).
2	`Time`	*Time* (64–bit floating point) Effective time of observation at $\varepsilon = 90°$ in International Atomic Time (TAI) seconds elapsed since 1981 January 1 00:00:00 UTC.[b]
3	`Photomet`	*Photometry* (32–bit floating point) Interpolated $\varepsilon = 90°$ intensity in MJy/sr.
4	`EfNumObs`	*Effective number of observations* (signed 16–bit integer) Approximate number of observations of the pixel over the mission (see FITS header for details).
5	`StdDev`	*Photometry standard deviation* (byte) Standard deviation of the interpolated intensity (`Photomet`) encoded as described in the FITS header.
6	`FitQual`	*Fit quality flag* (byte) Information about quality and type of interpolation to $\varepsilon = 90°$. Bit values indicate various conditions (see FITS header for details).
7	`FitChiSq`	*Fit* χ^2 (byte) χ^2 per degree of freedom for the interpolation.

[a] FITS keyword giving the label or heading for field (*i.e.*, table column) `n`.
[b] $T81$ (see §5.7.1.1). The quoted time, which is based on an interpolation of the observation times to $\varepsilon = 90°$, is not the same as the time at which the pixel center crossed $\varepsilon = 90°$. However the difference between these two times was typically less than 1 hour.

5.7.6 Galactic Plane Maps ($\varepsilon = 90°$)

The Galactic Plane Maps, which were designed to facilitate analysis of the Galaxy, are subsets of the $\varepsilon = 90°$ Sky Maps described in the previous section. Photometric data for all 10 *DIRBE* bands are given in a single 6 MB file. Each row of this FITS binary table corresponds to a *DIRBE* pixel. Table 5.7-12 describes the FITS table columns. More complete documentation is provided in the FITS header, which is listed in Appendix D.

Three versions of the Galactic Plane Maps file were produced. *The Pass 3B version supersedes both the initial DIRBE data product, which was released in July 1993 and prepared with an early version of the DIRBE data reduction software, and the Pass 2B version.* Over time, the calibration and map–making algorithms were refined. Early improvements compensated for the effect of photon–induced responsivity enhancement at 100 μm (see §3.4.2) and made beam offset corrections (see §4.2.2). Additional calibration changes, especially in the 1.25 – 12 μm bands, were introduced when the Pass 3B version was created.

With the following minor exceptions, the Pass 2B and 3B versions of the Galactic Plane Maps FITS file are identical in format to the Initial Product:

- the `PHOT_QUALITY` compression factor, N, used for the 12 and 25 μm bands (5 and 6) is 3 in the Initial Product and 4 in later versions, and

- the Pass 2B and 3B versions include a flag in bits 4–7 of the first `PHOT_QUALITY` byte indicating if an "outlier" weekly–average sample was excluded in the interpolation to $\varepsilon = 90°$.

The following section applies only to the (obsolete) Pass 2B version of the Galactic Plane Maps. Non–zero values are assigned to the FITS `TZERO` keywords in the Pass 3B version, and standard FITS ingest software should calculate the right ecliptic and Galactic coordinates.

Table 5.7-12: Columns in the Galactic Plane Maps FITS table

n	TTYPEn[a]	Description
1	`Pixel_no`	*DIRBE pixel number* (signed 32–bit integer) Pixel number in the CSC projection (see §5.3). Corresponding pixel center sky coordinates are given in columns 5,6,7 and 8.
2	`Photomet`	*Photometry* (vector of 10 32–bit floating point values) Intensity values for the 10 *DIRBE* photometric bands, in MJy/sr, listed in order of increasing wavelength.
3	`PhotQual`	*Quality of photometry* (vector of 10 signed 16–bit integers) Information about the quality of the photometric data. The first (least significant) byte indicates various conditions that affected the quality of the interpolation to $\varepsilon = 90°$; the standard deviation of the intensity is encoded in the second (most significant) byte. The 10 `PhotQual` values correspond respectively to the 10 `Photomet` values. See FITS header for interpretation instructions.
4	`TIME`	*Time* (64–bit floating point value) Effective time of observation at $\varepsilon = 90°$ in International Atomic Time (TAI) seconds elapsed since 1981 January 1 00:00:00 UTC.[b]
5	`EcLon`	*Ecliptic longitude* (signed 16–bit integer) J2000 ecliptic longitude of the CSC pixel center in degrees.
6	`EcLat`	*Ecliptic latitude* (signed 16–bit integer) J2000 ecliptic latitude of the CSC pixel center in degrees.
7	`GaLon`	*Galactic longitude* (signed 16–bit integer) Galactic longitude of the CSC pixel center in degrees.
8	`GaLat`	*Galactic latitude* (signed 16–bit integer) Galactic latitude of the CSC pixel center in degrees.

[a] FITS keyword giving the label or heading for field (*i.e.*, table column) `n`.
[b] $T81$ (see §5.7.1.1). The quoted time, which is based on an interpolation of the observation times to $\varepsilon = 90°$, is not the same as the time at which the pixel center crossed $\varepsilon = 90°$. However the difference between these two times was typically less than 1 hour.

5.7.6.1 Note on Quoted Coordinate Values (Pass 2B only)

Pixel center coordinates are represented as two–byte integers in the Galactic Plane Maps. Physical values will be reconstituted by generic FITS–reading software according to a transformation of the form physical value $=$ `TSCAL` $\times$ stored value $+$ `TZERO`. For all of the sky coordinates (`EcLon`, `EcLat`, `GaLon`, and `GaLat`), `TSCAL` was assigned the value $360/(2^{15}-1)$, corresponding to about a hundredth of a degree, in the FITS header. In each case `TZERO` was set to 0.

An offset *not* taken into account by `TZERO` should be added to the reconstituted coordinates to compensate for a bug in the software used to generate the integers recorded in the FITS file. Table 5.7-13 describes how the offset should be applied. The correction will automatically be applied by the *COBE* analysis software (see §D.1; version 3.0 or higher). The FORTRAN program `dirbe_gp_read` included in Appendix D also illustrates how the data should be treated.

Table 5.7-13: Offset values for Galactic Plane Map coordinates[a]

If the physical value in degrees is	Then add
value $\geqq 360/(2^{15}-1)$	$0.5 \times \left[360/\left(2^{15}-1\right)\right]$
value $\leqq -360/(2^{15}-1)$	$-0.5 \times \left[360/\left(2^{15}-1\right)\right]$
$-360/(2^{15}-1) < \text{value} < 360/(2^{15}-1)$	0.0

[a] Corrections applicable to `EcLon`, `EcLat`, `GaLon`, and `GaLat`.

5.7.7 Annual Average Sky Maps

The Annual Average Sky Maps are provided in 10 FITS binary table files, one per *DIRBE* intensity band. Both the file names and the FITS headers indicate to which band the data apply. Each row of the FITS table corresponds to a *DIRBE* pixel. Table 5.7-14 describes the FITS table columns. More complete documentation is provided in the FITS headers (see Appendix D for a sample header listing).

5.8 The Analyzed Science Data Sets

The Analyzed Science Data Sets (ASDS) are high–level products derived from reductions of the lower–level *DIRBE* data. Some of these data sets are by–products of the processing pipeline.

5.8.1 *DIRBE* Sky and Zodi Atlas and associated Pixel Index File

In many applications, the DSZA can be used instead of the DCAF. Most of the information in the DCAF is included in the DSZA, and the latter product also includes estimates of the zodiacal light intensity which can be compared directly with, or subtracted from, the *DIRBE* measurements. Using the DSZA, one can readily compare the apparent time variability of the sky, as observed by the *DIRBE* with that of the *DIRBE* IPD model (Kelsall *et al.* 1998), or construct sky maps like the ZSMA maps using different data selection criteria (*e.g.,* maps based on data obtained during different weeks in the cryogenic mission).

The DSZA is accompanied by a pixel index and organized in the same fashion as the DCAF (see §5.7.4). Table 5.8-1 lists the columns in the DSZA binary table. The data in columns 1–9 are identical to those in corresponding columns of the DCAF; the calculated zodiacal light intensity is given in column 10. The fields in the DSZA pixel index files are the same as those in the DCAF pixel index files (see Table 5.7-10). More detailed descriptions of the individual fields can be found in the FITS headers.

5.8.2 Zodi–Subtracted Mission Average Maps (ZSMA)

Like the Annual Average Sky Maps (see §5.7.7), the ZSMA Maps are provided in ten FITS binary tables, one each at 1.25, 2.2, 3.5, 4.9, 12, 25, 60, 100, 140 and 240 μm . The map wavelength is recorded both in the FITS header and the file name. Each row of the FITS table corresponds to a *DIRBE* pixel.

Table 5.7-14: Columns in the Annual Average Sky Map FITS tables

n	TTYPEn[a]	Description
1	`Pixel_no`	*DIRBE pixel number* (signed 32–bit integer) Pixel number in the CSC projection (see §5.3).
2	`PSubPos`	*Pixel sub–position* (byte) Gives the small offset between the centroid position of the samples included in the annual average and the pixel center coordinates (see §5.3).
3	`Time`	*Time* (64–bit floating point) Average of the times at which the pixel was observed during the entire cryogenic mission given in International Atomic Time (TAI) seconds elapsed since 1981 January 1 00:00:00 UTC.[b]
4	`Photomet`	*Photometry* (32–bit floating point) Average intensity observed for the pixel over the entire cryogenic mission, in MJy/sr.
5	`StdDev`	*Photometry standard deviation* (32–bit floating point) Standard deviation of the mean intensity (`Photomet`) in MJy/sr.
6	`WtNumObs`	*Weighted number of observations* (16–bit integer) Sum of the weekly weighted numbers of observations used to calculate the mean intensity, `Photomet`.
7	`SumNRecs`	*Total number of observations* (32–bit integer) Total number of times the pixel was observed during the mission, regardless of the weights assigned to the observations.

[a] FITS keyword giving the label or heading for field (*i.e.*, table column) `n`.
[b] $T81$ (see §5.7.1.1). *Note that the quoted time does not necessarily correspond to the time of an actual observation.*

Only one ZL–subtracted intensity value, representing an average over the cryogenic mission, is given per pixel.

Table 5.8-2 describes the data fields in the Zodi–Subtracted Mission Average maps. More detailed information is contained in the FITS header.

5.8.3 Photometric Standard Values Table

Photometric data obtained on 92 standard objects which were judged not to vary in brightness at a particular wavelength over the course of the cold mission were used to stabilize the *DIRBE* photometric system in the celestial calibration stage of the *DIRBE* data reduction pipeline (see Chapter 4). The Photometric Standard Values Table lists mission–averaged flux densities (in Jy) for the selected objects. The quoted flux densities assume a source spectrum characterized by νF_ν = constant (see § 5.5); a color correction (see Appendix B) must be applied to determine the true flux density if the source spectrum differs from the assumed energy distribution. Nominal wavelengths for the 10 *DIRBE* bands are 1.25, 2.2, 3.5, 4.9, 12, 25, 60, 100, 140 and 240 μm. The bandwidths and system responses at each wavelength are described in § 2.2.2, and the response functions are tabulated in Appendix A and provided as a data product (see § 5.9).

Like the other calibrated *DIRBE* products, the Photometric Standard Values Table quotes flux densities whose absolute calibration at each wavelength is based upon measurements of a single source (see § 4.5.3). The *DIRBE* point source photometry agrees with that of Engelke (1992) and Cohen *et al.* (1992, 1995) at 2.2 μm and 12 μm (*IRAS*) to within the absolute calibration uncertainties of the different systems.

The quoted flux densities were derived as follows. For individual sightings of the standard objects in the time–ordered data, a local background intensity and a background–subtracted flux density were calculated using the algorithm described in § 4.5.3.2. At each wavelength, the background–subtracted flux densities were then averaged over the cold mission. The quoted error is the standard deviation of

Table 5.8-1: Columns in the DIRBE Sky and Zodi Atlas

n	TTYPEn[a]	Description
1	`Pixel_no`	*DIRBE pixel number* (signed 32–bit integer) Pixel number in the CSC projection (see §5.3).
2	`Time`	*Time* (64–bit floating point) Average of the times at which the pixel was observed during the week given in International Atomic Time (TAI) seconds elapsed since 1981 January 1 00:00:00 UTC[b].
3	`DeltaT`	Δ*Time* (vector of 10 bytes) Since the number of measurements included in a weekly average was photometric band–dependent, the `Time` value is only an approximation to the average time the pixel was observed at a particular wavelength. A more accurate time for each band is `Time` plus the value of `DeltaT` for that band.
4	`SolElong`	*Solar elongation angle,* ε (signed 16–bit integer) Average of the solar elongation angles at which the pixel was observed during the week. The comment made about the accuracy of `Time` under `DeltaT` also applies to `SolElong`.
5	`Photomet`	*Photometry* (vector of 10 32–bit floating point values) Average intensity observed for the pixel over the week, in units of MJy/sr. The 10 values correspond to the 10 *DIRBE* bands in order of increasing wavelength.
6	`NumRecs`	*Number of records* (signed 16–bit integer) Number of times the pixel was observed this week in at least one photometric band. (Observations made contemporaneously at multiple wavelengths count once.)
7	`WtNumObs`	*Weighted number of observations* (vector of 10 bytes) Number of observations that survived robust averaging and quality constraints and were used to form the average intensity values given in the `Photomet` field. Listed in order of increasing wavelength.
8	`StdDev`	*Photometry standard deviation* (vector of 10 bytes) Standard deviations of the mean weekly intensities for the 10 *DIRBE* bands given in ascending wavelength order and encoded. The FITS header describes how to decode the stored values.
9	`SSOFlag`	*Solar system object flag* (byte) Indicates which solar system object exclusion zones (see §5.6.2), if any, intersect the pixel at some time during the week. See FITS header for interpretation instructions.
10	`ZL`	*Zodiacal Light* (vector of 10 32–bit floating point values) Brightness of the zodiacal light, in units of MJy/sr, as computed from the DIRBE IPD Model for the time of observation (`Time` + `DeltaT`) and pixel coordinates. The 10 values correspond to the 10 *DIRBE* bands in order of increasing wavelength.

[a] FITS keyword giving the label or heading for field (*i.e.*, table column) `n`.
[b] *T*81 (see §5.7.1.1).

Table 5.8-2: Columns in the Zodi–Subtracted Mission Average Maps

n	TTYPEn[a]	Description
1	`Pixel_no`	*DIRBE pixel number* (signed 32–bit integer) Pixel number in the CSC projection (see §5.3).
2	`Resid`	*Residual intensity* (32–bit floating point) Unweighted average of weekly ZL–subtracted intensity values over the entire cryogenic mission, in MJy/sr.
3	`NumObs`	*Number of Observations* (signed 32–bit integer) The total number of individual photometric measurements included in the average.
4	`NumWks`	*Number of weeks* (8–bit byte) The number of weekly averaged intensity values used to compute the mission averaged residual intensity. This number varies with location in the sky.
5	`StdDev`	*Standard deviation* (32–bit floating point) Standard deviation of the mean ZL–subtracted intensity (`Resid`) in MJy/sr.

[a] FITS keyword giving the label or heading for field (*i.e.*, table column) `n`.

the mean flux density value; it *does not include the absolute calibration uncertainty.* When values of 0.0 are given for the flux density and error at a particular wavelength, they indicate that the object was not an approved calibration source at that wavelength.

To have been selected as an approved calibration object, a source had to satisfy the following criteria: little ($\lesssim$ 2%) or no variability was seen in the photometry over the course of the cold mission; and the signal–to–noise ratio for a typical sighting was $\geq$ 20 for 1.25 - 4.9 μm, or $\geq$ 10 for 12 - 240 μm. The histograms in Figure 5.8-1 show the calibrator flux density ranges at the 10 *DIRBE* wavelengths; the labels tell how many sources qualified as calibrators. Few sources qualified at the longer wavelengths.

A background intensity value, in MJy/sr, is provided in the Photometric Standard Values Table at each wavelength for which the object was approved as a calibrator. The background values can be used to assess the source–to–background contrast if the beam solid angles given in Table 4.2-1 are used to convert the intensity units from MJy/sr to Jy/beam. Note that the listed background intensity is an average over individual sightings within the mission; the intensity actually detected varied as a function of time as the source was seen along different lines of sight through the interplanetary dust.

The coordinates of the objects are given in the equatorial (epoch 1950), Galactic, and geocentric ecliptic (epoch 2000) systems, and the data are tabulated in order of increasing Right Ascension. Figures 5.8-2 and 5.8-3 show the locations of the calibration sources in Galactic and ecliptic coordinates, respectively. Objects at ecliptic latitudes $|\beta| \gtrsim 65°$ are visible throughout the entire mission; the visibility decreases at lower latitudes. Most of the source positions provided for 1.25 – 25 μm calibrators are taken from the SAO Bright Star Catalog (available from the Astronomical Data Center at `ftp://adc.gsfc.nasa.gov/pub/adc/archives/catalogs/5/5050/`). *IRAS* Point Source Catalog (PSC; see `http://www.gsfc.nasa.gov/astro/iras/psc.html`) positions were used for some circumstellar dust sources that did not appear in the SAO catalog. At the longer wavelengths (60 – 240 μm), source positions were taken from (in order of preference) the *IRAS* PSC, the *IRAS* Small Scale Structure Catalog (see `http://www.gsfc.nasa.gov/astro/iras/sss.html`), or the *DIRBE* time–ordered data themselves. In the latter cases, positional errors may be as large as a few arcminutes.

As a rule, but with some exceptions, stellar objects are referred to by a constellation designation (*e.g.,* YY Psc); Sharpless numbers are used for H II regions (*e.g.,* S 140); and NGC or Messier numbers are used for galaxies (*e.g.,* NGC 253).

Table 5.8-3 describes the format of the Photometric Standard Values Table.

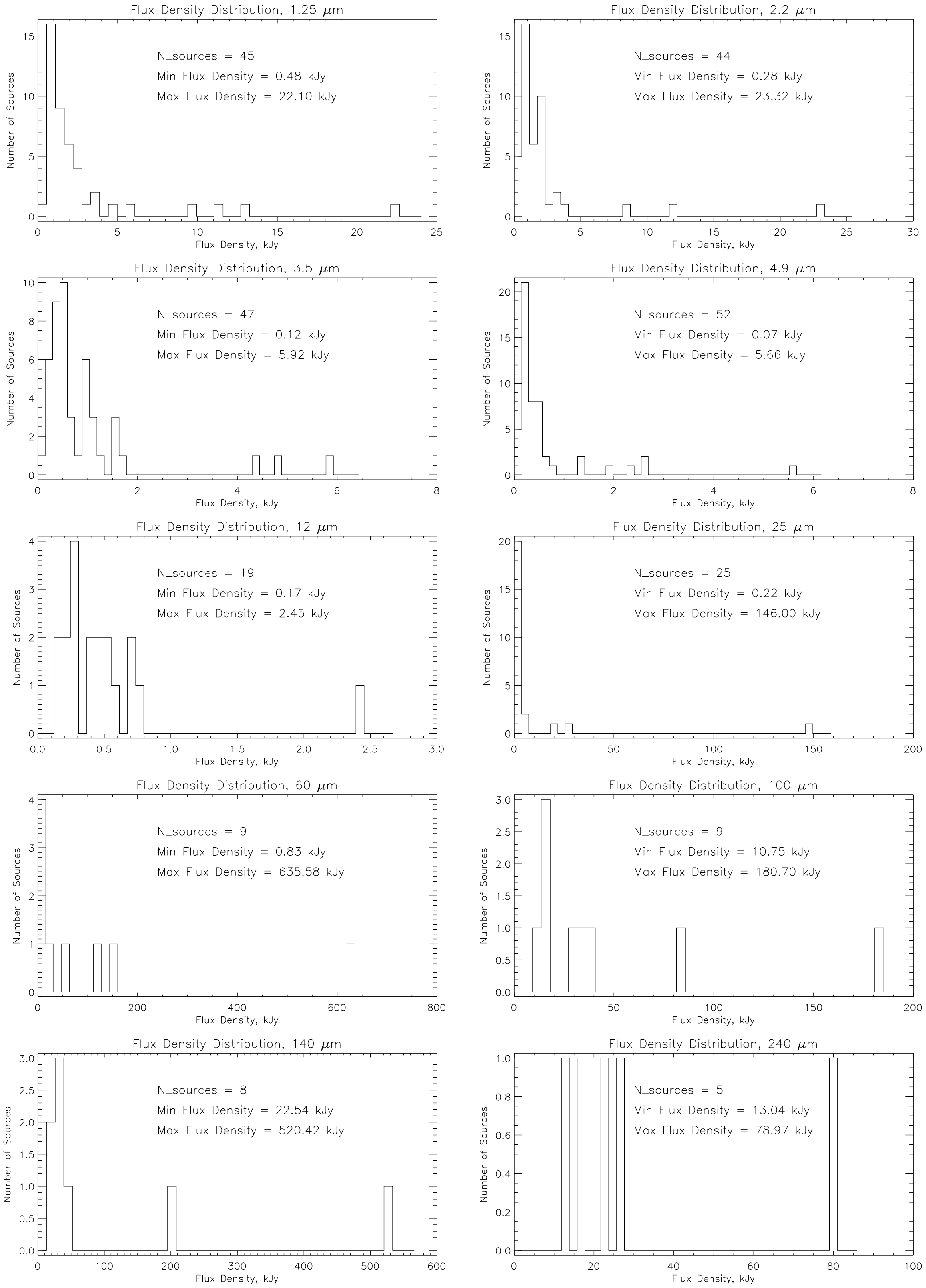

Figure 5.8-1: Histograms of the flux densities of sources used as relative calibrators for each of the ten *DIRBE* bands.

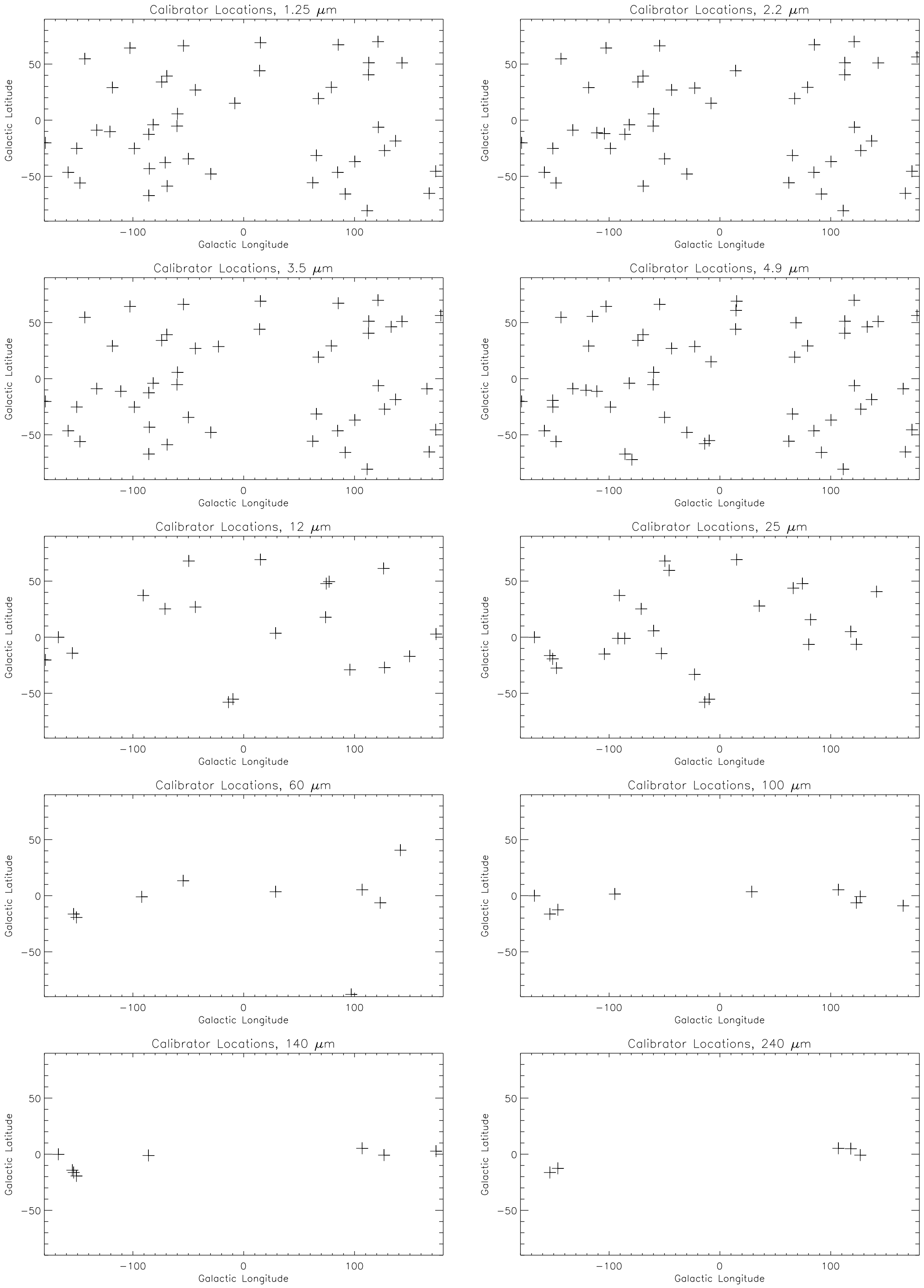

Figure 5.8-2: Locations of the relative calibration sources in Galactic coordinates.

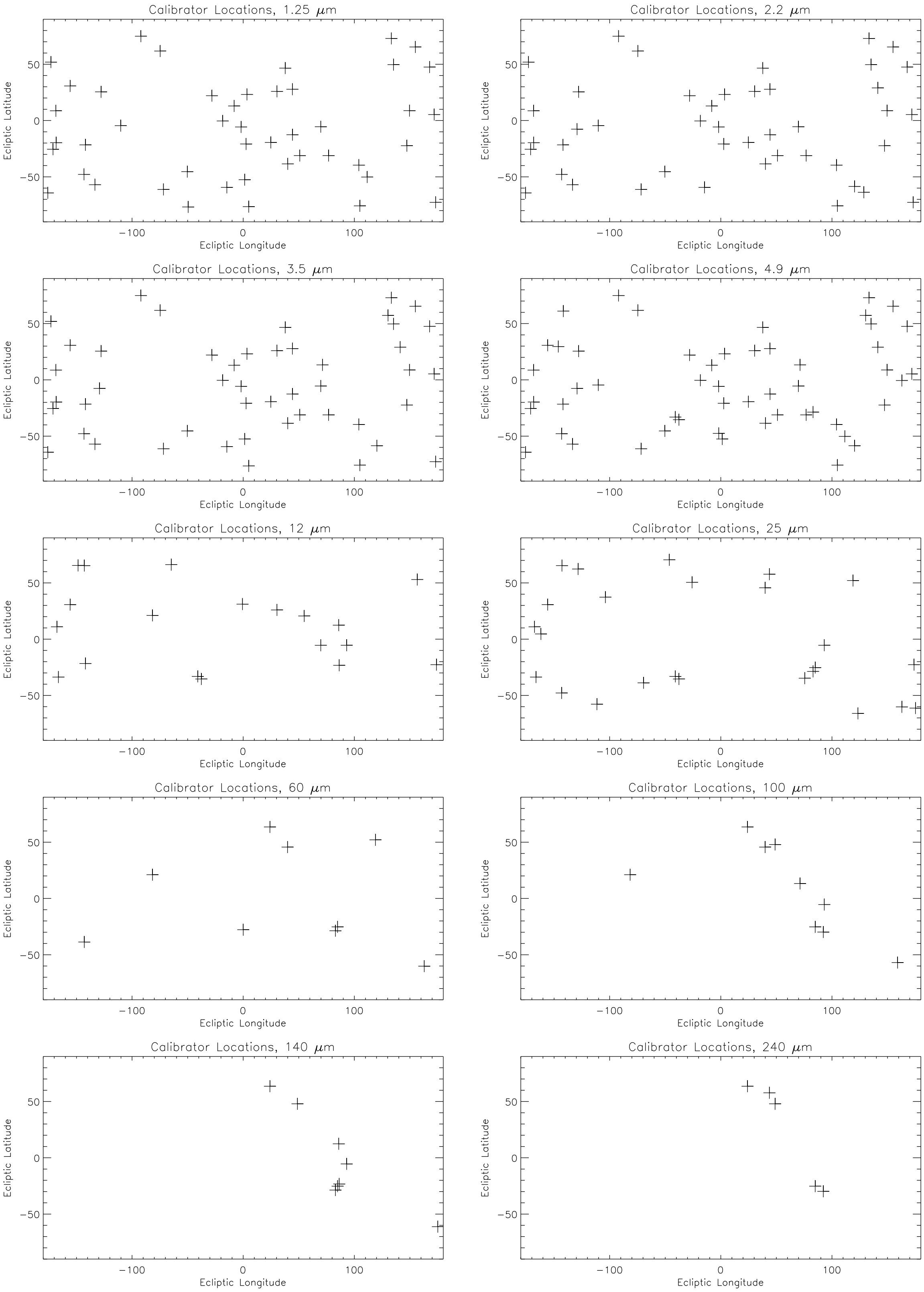

Figure 5.8-3: Locations of the relative calibration sources in geocentric ecliptic coordinates.

Table 5.8-3: Columns in the Photometric Standard Values Table

n	TTYPEn[a]	Description
1	`Name`	*Object name* (32–bit character) Name of the calibration object.
2	`ObjIndex`	*Object index* (signed 16–bit integer) DIRBE object index number.
3	`Pixel_No`	*DIRBE pixel number* (signed 32–bit integer) DIRBE pixel in which the object is located.
4	`RA1950`	*Right Ascension* (32–bit floating point) Right Ascension of the object, epoch 1950, in decimal hours.
5	`DEC1950`	*Declination* (32–bit floating point) Declination of the object, epoch 1950, in decimal degrees.
6	`GalLon`	*Galactic longitude* (32–bit floating point) Galactic longitude, ℓ_{II}, of the object, in decimal degrees.
7	`GalLat`	*Galactic latitude* (32–bit floating point) Galactic latitude, b_{II}, of the object, in decimal degrees.
8	`EclLon`	*Ecliptic longitude* (32–bit floating point) Ecliptic longitude of the object, epoch 2000, in decimal degrees.
9	`EclLat`	*Ecliptic latitude* (32–bit floating point) Ecliptic latitude of the object, epoch 2000, in decimal degrees.
10	`Photomet`	*Average photometry* (10 32–bit floating point) Mission–averaged background–subtracted flux densities, in units of Jy, listed in order of increasing wavelength from 1.25 to 240 μm. Flux densities are quoted at the nominal wavelength for a source with νF_ν = constant (a color correction is required if the true source spectrum differs from the assumed shape).
11	`StdDev`	*Standard deviation* (10 32–bit floating point) Standard deviation of the mean flux density quoted in the corresponding *Average photometry* field, in Jy (*i.e.,* one value per wavelength band, listed in order of increasing wavelength).
12	`NumObs`	*Total number of observations* (10 32–bit integer) The total number of individual observations used to derive the flux density quoted in the corresponding *Average photometry* field (*i.e.,* one value per wavelength band, listed in order of increasing wavelength).
13	`AvgBkgd`	*Average background* (10 32–bit floating point) Average background intensity, in MJy/sr, at each wavelength, listed in order of increasing wavelength.

[a] FITS keyword giving the label or heading for field (*i.e.*, table column) `n`.

5.8.4 Solar System Object Data

The Solar System Object Dataset provides flux densities and other data pertaining to individual passages of solar system objects through the *DIRBE* field of view during the period of cryogenic operation, from 11 December 1989 to 21 September 1990. The data are given in FITS tables, one for each of the following objects: Mars, Jupiter, Saturn, Uranus, Ceres, Pallas, and Vesta. Due to their low solar elongation angles, Mercury and Venus were not visible to the *DIRBE* , the Moon saturated the *DIRBE* detectors, and other solar system objects were generally below the source detection thresholds discussed below. Each table contains one record per object passage, and the sightings are organized chronologically. The FITS table columns are described in Table 5.8-5.

An object was considered to have been detected, and a table entry was made, only if a point source signal was evident in the time–ordered data. A zero–sum filtered data stream was checked for signals in at least two detectors in excess of specified detection thresholds. The filter–weighted signal was obtained by multiplying 9 consecutive $\frac{1}{8}$–second data samples by the factors -1, -1, -1, 2, 2, 2, -1, -1, -1 and summing the result. The detection thresholds used were equivalent to the point source flux density values listed in Table 5.8-4. Where confusion noise is negligible, the detection thresholds correspond to signal–to–noise ratios of about 20 for detectors 1A–4, 8 for detectors 5–7, and 10 for detectors 8–10.

Table 5.8-4: Solar System Object Detection Thresholds

Wavelength (μm)	1.25	2.2	3.5	4.9	12	25	60	100	140	240
Detector	1A	2A	3A	4	5	6	7	8	9	10
Threshold (Jy)	140	120	78	96	130	270	380	590	40000	20000

Positional criteria were used to further guard against the inclusion of low quality data. First, at the time of the object's closest approach to the center of the field of view, its ephemeris position was required to lie within $\pm 10'$ of the *DIRBE* boresight position in the in–scan direction, and within $\pm 18'$ in the cross–scan direction. Second, any data obtained while the *DIRBE* boresight passed within $60'$ of either a *DIRBE* approved calibration object or another solar system object were excluded. Objects other than these, which could potentially contaminate the photometry, were *not* checked for positional coincidence.

Source photometry was calculated from the time–ordered data as follows:

1. A 15–point string of data was extracted, centered on the time of the object's closest approach to the center of the field of view;

2. a linear (for Bands 1-4) or quadratic (for Bands 5-10) function was fitted to the off–source region of the data string (typically the first 6 and the last 6 data samples) and used as a background model;

3. according to the cross–scan position of the object, a beam profile response template (*i.e.,* response as a function of in–scan position) was selected. The beam templates were derived from the normalized beam profile maps described in §5.9.1);

4. the portion of the background–subtracted intensity profile corresponding to the passage of the source through the beam – typically the 3 central data points – were fitted to the beam template times a constant factor. This factor is the point source flux density in instrument DNs.

5. Finally, this measure of the flux density was scaled by the appropriate celestial and absolute calibration coefficients (see §4.5.3), yielding the flux density value, in Jy, which is given in the `Photomet` field in the Solar System Object Dataset.

According to our convention, the quoted flux density corresponds to that of a source having a spectral shape $\nu F_\nu = constant$. Thus a color correction (see Appendix B) must be applied to obtain the true flux density if the real spectrum has a different shape, as is typically the case.

The photometry from a particular detector was considered unreliable if there were large residuals about the background or beam template fits, or if the object passed close to the "edge" of the beam, where pointing error would result in a large uncertainty in the adopted beam template. In such cases, a sentinel value (-16000.) is recorded in the `Photomet` and `PhotErr` fields for the affected detector.

Positions of Mars, Jupiter, Saturn and Uranus were computed using the method of van Flandern and Pulkkinen (1979). Coordinates for the asteroids (Pallas, Ceres, Vesta) were calculated with a routine provided by M. A'Hearn (University of Maryland), using the orbital elements listed in Table 5.8-6.

5.8.5 Faint Source Model (FSM)

The *DIRBE* Faint Source Model, which was used by Arendt *et al.* (1998) to subtract (faint) stellar emission from the *DIRBE* sky maps as part of the search for the cosmic infrared background, is available as a data product. A detailed description of the Faint Source Model, and warnings with which the user should be familiar, can be found in Appendix F.

For each step along a line of sight, the FSM was used to compute an intensity and a variance in intensity at 1.25, 2.2, 3.5, 4.9, 12 and 25 μm . Assuming Poisson statistics, the variances are proportional to the number of sources in each volume element. The intensities and variances are integrated over distance, source type, and Galactic structure component (see Appendix F). The square root of the total variance for each line of sight gives the 1σ uncertainty assigned to the intensity in the corresponding *DIRBE* pixel. As shown in Table 5.8-7, the predicted intensities and their associated uncertainties are recorded in the FSM data product. There are six FSM FITS binary tables, one per wavelength. Each file is 5 MB in size.

5.9 Ancillary Data Sets

Machine–readable files containing important calibration information given in the *Explanatory Supplement* are included among the *DIRBE* data products.

5.9.1 Beam Profile Maps

Beam Profile Maps are provided in 16 FITS image files, one for each of the *DIRBE* detectors. Both the file names and the FITS headers indicate to which band the data apply. A sample FITS header is given in Appendix D. Each map is a 225 (in–scan) $\times$ 181 (cross–scan) pixel array with $0.4'$ pixel spacing in the cross–scan direction and $0.375'$ sampling in the scan direction.[2] The array values give the beam response normalized to unity at the peak.

Beam profiles for 10 of the detectors (bands 1A–4) were found to vary slightly over time, while those for bands 5–10 were taken to be constant throughout the cryogenic mission. Three separate beam profiles are given for the short–wavelength bands, one applicable to the time interval 89345 – 90176, another to 90176 – 90232, and a third to 90232 – 90264. The beam solid angles are listed in Table 4.2-1 and given in the FITS headers. The tabulated solid angles were used in the *DIRBE* data reduction software to convert the detected flux per beam into intensity in MJy/sr.

5.9.2 Spectral Response Functions

The *DIRBE* System Spectral Response functions depicted in Figure 2.2-2 and tabulated in Appendix A are also provided in an ASCII file called DIRBE_SYSTEM_SPECTRAL_RESPONSE_TABLE.ASC.

An early version of the file reported wavelengths to the nearest hundredth of a micron and contained what appeared to be duplicate entries at 1.00, 1.04, 1.09 and 1.16 μm. A new version of the table released in March 1997 quotes wavelengths to the nearest 0.001 μm and does not contain duplicate entries. The responsivity values are the same in both versions of the table.

5.9.3 Color Correction Tables

Color correction factors applicable to spectral energy distributions of the following forms are tabulated in Appendix B and provided in an ASCII file called DIRBE_COLOR_CORRECTION_TABLES.ASC: $I_\nu \propto$

[2] The now–obsolete Pass 2B Beam Profile Maps were more coarsely sampled.

Table 5.8-5: Contents of Solar System Object Dataset

n	TTYPEn[a]	Description
1	`Time`	*Time of closest approach* (64-bit floating point) Time of the object's closest approach to the center of the field of view, in TAI seconds since 1981 January 1 00:00:00 UTC[b].
2	`Pixel_No`	*DIRBE pixel number* (signed 32–bit integer) Pixel in the CSC projection (see §5.3) in which the object is located at the time recorded in the `Time` field.
3	`RA1950`	*Right Ascension* (32-bit floating point) Coordinate of the object at the time recorded in the `Time` field, in hours, epoch 1950.
4	`DEC1950`	*Declination* (32-bit floating point) Coordinate of the object at the time recorded in the `Time` field, in decimal degrees, epoch 1950.
5	`GalLon`	*Galactic longitude* (32-bit floating point) Coordinate of the object at the time recorded in the `Time` field, in decimal degrees.
6	`GalLat`	*Galactic latitude* (32-bit floating point) Coordinate of the object at the time recorded in the `Time` field, in decimal degrees.
7	`EclLon`	*Ecliptic longitude* (32-bit floating point) Coordinate of the object at the time recorded in the `Time` field, in decimal degrees, epoch 2000.
8	`EclLat`	*Ecliptic latitude* (32-bit floating point) Coordinate of the object at the time recorded in the `Time` field, in decimal degrees, epoch 2000.
9	`SolElong`	*Solar Elongation* (32-bit floating point) Solar Elongation angle of the object at time recorded in the `Time` field, in decimal degrees
10	`Distance`	*Geocentric distance* (32-bit floating point) Distance of the object from Earth at the time recorded in the `Time` field, in Astronomical Units.
11	`HelioDist`	*Heliocentric distance* (32-bit floating point) Distance of the object from the Sun at the time recorded in the `Time` field, in Astronomical Units.
12	`Photomet`	*Flux density* (vector of 10 32–bit floating point values) Flux density of the object in the ten *DIRBE* total intensity wavelength bands, in Jy, listed in order of increasing wavelength from 1.25 to 240 μm . Color corrections may be required (see text).
13	`PhotErr`	*Photometric uncertainty* (vector of 10 32–bit floating point values) Estimated error in the flux density, in Jy. Calculated as the quadrature sum of (1) the rms deviation of the time–ordered data from the baseline and beam template fits, and (2) the error due to uncertainty in the beam template associated with cross–scan pointing error.

[a] FITS keyword giving the label or heading for field (*i.e.*, table column) `n`.
[b] $T81$ (see §5.7.1.1).

Table 5.8-6: Orbital elements used to calculate asteroid ephemerides

	Pallas	Ceres	Vesta
Perihelion date (yrs)	1986.244072	1986.074926	1989.314116
Perihelion distance (AU)	2.1201106	2.552557	2.1473662
Eccentricity	0.2347	0.0780	0.0906
Argument of perihelion (deg)	309.796	71.274	150.175
Ascending Node (deg)	173.323	80.702	104.015
Inclination to Ecliptic (deg)	34.804	10.607	7.139
Epoch (yrs)	1989.751	1989.751	1989.751
Equinox (yrs)	2000.0	2000.0	2000.0

Table 5.8-7: Columns in the Faint Source Model FITS tables

n	TTYPEn[a]	Description
1	`Pixel_no`	*DIRBE pixel number* (signed 32–bit integer) Pixel number in the CSC projection (see §5.3).
2	`Photomet`	*Photometry* (32-bit floating point value) Faint Source Model intensity in MJy/sr.
3	`StdDev`	*Standard deviation* (32-bit floating point value) Standard deviation of the intensity (`Photomet`) in MJy/sr.

[a] FITS keyword giving the label or heading for field (*i.e.*, table column) `n`.

ν^n, where $n = -3.0, -2.5, -2.0, \ldots, +3.0$; and $I_\nu \propto \nu^n B_\nu(T)$, where $n = 0.0, 0.5, \ldots, 2.0$, temperature T is in the range $[10\mathrm{K}, 20000\mathrm{K}]$, and $B_\nu(T)$ is the Planck function.